NOAA CRCP NA18NOS4820113
Final Report

1. Date: June 17, 2021

2. Project PI & contact information:

Dr. David Eggleston & Dr. Del Bohnenstiehl
North Carolina State University
Department of MEAS
2800 Faucette Drive
Raleigh NC 27695
919-515-7840, eggleston@ncsu.edu; 919-515-7449, drbohnen@ncsu.edu

3. CFDA Number: 11.482

4. Type of report: Final Report for CRCP NA18NOS4820113

5. Reporting Period: 08/01/2018-12/31/2020

6. Project Summary

a. Title: Integrating Visual Ecological Surveys, Passive Acoustics and Habitat Photogrammetry to Characterize Reef Fish Assemblages, Spawning Activity & Resilience Among Management Zones in the FKNMS Post-Hurricane Irma

b. Priorities Addressed: (1) Fish Impacts-National: Projects to obtain essential life history and ecological information on key coral reef fisheries species or functional groups; (2) ESA-National (Atlantic/Caribbean): Projects that support the recovery of key foundational corals (e.g. *Acropora* and *Orbicella* species) listed as threatened under the ESA; (3) Climate Change-National: Projects that implement management actions identified through the reef resilience and vulnerability assessment in project jurisdiction.

c. Summary: This project used a multidisciplinary approach to quantify reef fish species composition, reef structural complexity and habitat associations among the various management zones (Sanctuary Preservation Areas, SPA; Special Use, Research Only Areas, SUA; Ecological Reserve, ER SPA; and Open to fishing, no management designation) in the lower (Zone D) Florida Keys National Marine Sanctuary (FKNMS) (Table 1; Figure 1). Methods included a combination of visual surveys, passive acoustic monitoring, and habitat mapping using visual survey techniques, as well as relatively novel habitat photogrammetry techniques. The data and results are providing fine-scale information among the various management zones on: (i) coral assemblages and their contribution to habitat complexity, (ii) fish density and diversity, (iii) the underwater soundscape, and (iv) resilience of the coral reef soundscape to hurricane impacts.

d. Issues & Solutions: The number of sites sampled using underwater hydrophones per deployment varied because hydrophones were either removed by unknown divers or was not found after passage of Hurricane Irma. Poor weather conditions and/or low visibility precluded visual surveys at certain times and sites. Five reef sites (Sand Key, Nine Foot

Stake, Western Sambo, Eastern Sambo, Looe Key SPA) were successfully mapped using Structure-from-Motion (SfM) photogrammetry to resulting in high-resolution (i) digital elevation models, and (ii) orthomosaics. The lack of spatial coverage and camera quality hindered SfM mapping of Western Dry Rocks and Looe Key SUA.

e. Accomplished Work:

Research trips. – A total of eight Reef Visual Census (RVC) survey field trips were conducted between February 2017 and December 2018. The RVC surveys quantified reef fish and habitat characteristics. Bottom-mounted hydrophones were deployed during each survey--hydrophones already deployed were retrieved on subsequent trips and replaced with hydrophones containing fresh batteries and data storage cards.

Publications. – The manuscript "Hurricane impacts on a coral reef soundscape" is available via open access: https://doi.org/10.1371/journal.pone.0244599. The accompanying dataset is available for access via https://doi.org/10.5061/dryad.5tb2rbp38. NC State's College of Science communications office has featured this publication in their press release, and the story was picked-up by BBC and Popular Science magazine. We are actively preparing additional manuscripts for publication from the various datasets collected during this study.

Conferences & Presentations

1. Simmons K. Oral presentation. Hurricane impacts on a coral reef soundscape. Southeast Climate Adaptation Science Center – Global Change Seminar Lightening Talk. Raleigh NC. Sept 2019.
2. Simmons K, Bohnenstiehl D, Eggleston D. Oral presentation. How did Hurricane Irma affect the underwater soundscape in the Florida Keys. Association for the Sciences of Limnology & Oceanography (ASLO) Conference San Juan, Puerto Rico. Feb 2019
3. Simmons K, Bohnenstiehl D, Eggleston D. Oral presentation. Evaluating the Efficacy of Management Zones in the FKNMS: Integrating Visual Surveys, Habitat Data, and Passive Acoustics to Monitor Reef Fish Assemblages and Spawning Activity. World Conference for Marine Biodiversity (WCMB), Montreal, Quebec Canada, May 2018.

Outreach

1. Featured on NOAA ONMS Sanctuary Sound Monitoring "SanctSound FKNMS Story Map" https://sanctuaries.noaa.gov/science/monitoring/sound/sanctsound-storymap.html (in prep)
2. Kayelyn Simmons volunteered with non-profit organization CESAM (Capitulo Estudiantil de la Sociedad Ambiente Marino) to recover and restore fragmented Acropora spp. on impacted reefs due to Hurricane Maria's tract across San Juan, PR in 2019.
3. In 2018, an outreach event entitled "Coral Reef Soundscape Block Party" took place in collaboration with Divers Direct Dive Shop in Key West (John Hadfield, store manager), the NOAA-CRCP (Robin Garcia, Communications Director), the NOAA/ONMS FKNMS (Gena Parsons, Communications/Outreach Manager), NC State College of Sciences, and several local Key West dive shops.

f. Report Results/Findings

Introduction – Comparisons between the diverse spatial management zones and non-regulated sites within the Florida Keys National Marine Sanctuary (FKNMS) network of 18 "no-take" Sanctuary Preservation Areas (SPAs), one "no-take" Ecological Reserve (ER), and four Special Use Areas (SUAs) can be used to address fundamental questions regarding some of the drivers of biodiversity and habitat complexity, and the implications of such features on resilience of coral reef systems to anthropogenic and natural stressors. In the wake of Hurricane Irma in the fall of 2017, these sites can also be used to understand the extent to which biodiversity influences recovery from perturbations. It is often assumed that more diverse ecosystems are more resilient to change (e.g., McClanahan et al 2012); yet there is considerable debate in the contemporary literature on whether or not this assumption is generally true (NRC 2015). Resolving the interplay between biodiversity and ecosystem resilience, while a daunting challenge, is essential for understanding the cumulative and individual effects of changes related to Earth's climate, resource use and extraction, as well as management efforts aimed at restoring or enhancing ecosystems. Moreover, defining ecological units to assess impacts for local and regional management plans can be difficult when spatiotemporal differences occur at complex scales. For example, seascape-level metrics relevant to ecological resilience, such as coral cover and diversity or herbivorous fish biomass are often important at local spatial scales (Goergen et al. 2020; Shaver et al. 2020 and references therein).

According to the FKNMS Science Plan 2002 and the NOAA-CORIS Florida Reef Resilience report, resource managers require up-to-date, high-resolution data on reef fish biodiversity, coral species conditions, impact responses, and resiliency indicators to guide decision-making and prioritize actions that support resiliency. A comprehensive study examining reef fish biodiversity and habitat associations as a function of management, however, has not been conducted in the FKNMS since 2004. Beginning February 2017, we collected data on (i) reef fish, (ii) habitat, and (iii) underwater soundscapes at the proposed study sites using the methods described below. Given the direct impact of Hurricane Irma on our study sites in the FKNMS, specifically fore-reef habitats characterized by relatively high resilience (Maynard et al. 2017), rapid reef assessments and emergency restoration efforts are now being implemented by NOAA and the State of Florida—the completed research should help inform those efforts.

Overview of Methods & Results - In the sections below, we provide an overview of Methods and Results for the following objectives: (1) Reef composition and habitat complexity, (2) Reef fish distribution, abundance and diversity, (3) Spatiotemporal variation in the underwater soundscape, and (4) Impact of hurricane Irma on the underwater soundscape. We emphasize that in addition to the publication from this project on the impact of hurricane Irma on the coral reef soundscape (Simmons et al. 2020), we will continue to actively analyze data and generate manuscripts for submission to peer-reviewed journals.

(1). Characterize Reef Composition & Habitat Complexity **–** Efforts to understand and monitor spatiotemporal variation across reef habitats recognize the need for spatially relevant metrics and biological data at multiple scales (e.g., organism level to community level) (Pittman et al. 2021). The use of fine-scale mapping tools such as Structure-from-Motion (SfM) photogrammetry is

becoming widely used to monitor and quantify differences among sites that vary in three-dimensions (Ferrari et al. 2016; Burns et al. 2019). These fine-scale reef mapping approaches also capture local variability in biotic cover and relevant physical features at the colony scale (1mm -1cm pixel) which is often appropriate for local management priorities (Phinn et al. 2012; Royer et al. 2018).

We used visual habitat surveys and a sub-set of high resolution reef maps produced by SfM photogrammetry of coral reefs located in different management zones within the Florida Keys National Marine Sanctuary, USA to characterize spatiotemporal variation in coral reef habitat features relevant to benthic communities and reef structure. We also compared and contrasted changes in habitat characteristics before versus after the passage of Hurricane Irma (September 2017) in the Lower Keys section of the FKNMS. Reef Visual Census (RVC) surveys were conducted seasonally by scuba divers at eight fore-reef study sites in the lower Florida Keys between February 2017 – December 2018 (Figure 1; Table 1). In 2018, SfM habitat photogrammetry was conducted within a subset of 5 of 8 sites (Figure 2). The general approach included generating a suite of statistically independent habitat metrics from each data source (i.e., RVC vs SfM) to test for differences in habitat characteristics among sites and over time. These datasets were also used to observe differences in metrics derived from each data source. The results from the present study may serve as a baseline for a more fine-scale approach to long-term monitoring and restoration efforts by characterizing the relationship between management zones, coral reef assemblages and habitat characteristics on a local scale.

Methods

Reef Visual Census (RVC) – Reef Visual Census (RVC) surveys followed standardized protocols developed by a cooperative multi-agency network of the Florida Fish and Wildlife Conservation Commission (FWCC), NOAA, National Park Service, and the University of Miami (Brandt et a. 2009). Primary sampling units (100 x 100m cells) within in each reef site were generated and further subdivided into a two-stage stratified random design in which two divers conducted a 15-minute reef visual census survey inside a 15m diameter cylinder. The surveys from the two divers were non-overlapping (~ 10-30 m apart), and the data from the divers combined to produce mean values for many of the habitat characteristics within a given monthly survey at a given site. Thus, the sample size for each site was four for Pre-Irma (Feb., May, July, Dec., 2017) versus four post-Irma surveys (Feb., Jan., Sept., Dec., 2018). Visual surveys by divers generated information on (i) depth(m), (ii) hard relief (m) of stony corals), (iii) soft relief (m) of soft corals, (iv) abiotic footprint (% sand, hardbottom, rubble), and (v) the dominant biological cover of the hardbottom (% algae, live stony corals, octocorals, sponges) (Table 3a).

Structure-from-motion (SfM) – Structure-from-motion photogrammetry surveys were completed three GoPro-Hero3/Hero 4 cameras mounted on a PVC frame and position to provide ~70% overlap in the across-track direction. The cameras were programmed to collect digital still images every 2 seconds as the diver swam back and forth across the reef. To constrain the scale in these models fixed-length T-sticks were deployed adjacent to key habitat features, and up to six ground control points (GPCs) were established within each site. Images were processed using Agisoft Metashape (v 1.5.2.7838) SfM software following the workflows from similar studies, such as Burns et al. (2015, 2019) and Fukunaga et al. (2019). Initial photo alignment settings used a key point limit and tie point limit of 40,000 and 10,000, respectively, with the

level of accuracy set as 'High' and generic preselection enabled. Next, a dense elevation point cloud was generated and used to create digital elevation models (DEMs). All DEMs were exported at ~0.5cm pixel resolution as GeoTIFF files with both local and UTM coordinates. Imagery from Western Dry Rocks and Looe Key SUAs were not successful in the image alignment process due to poor visibility and/or lack of sufficient overlapping images.

Digital Elevation Model (DEM) – The DEMs were imported into ArcGIS Pro to quantify habitat complexity metrics using the 3D Analyst and Spatial Analyst and Benthic Terrain Modeler (BTM) v3.0 to obtain habitat metrics such as average depth, slope, vector ruggedness measure (VRM), as well as the surface area-to-planar area ratio (See Table 3b). Slope values were derived from a geodesic plane using 3x3 neighborhood scales to measure the angle between surface and local *z-y-z* coordinates across adjacent cells. The surface area to-planar (sapa) ratio is an analogous metric to the more commonly used rugosity ratio, and also uses a 3x3 neighborhood window in which the center of each central cell is split into three dimensions or eight triangles to calculate the contoured surface of each cell location, thereby giving the sum area of the network of triangles divided by the slope. The DEMs and derived raster layers were then imported into MATLAB, where they were sampled along a series of transects, or scanlines, orthogonal to the spur and grove terrains. Each transect was 30m in length with a 3m spacing in between each transect. Additional scanline metrics calculated include the relief, root mean square (rms) roughness and rugosity of each topographic profile (e.g., Nunes & Pawlak 2008; Bozec et al. 2015; Aronson & Precht 1995; Alvarez-Filip et al. 2011; Young et al. 2017).

Characterizing Coral Assemblages – To further characterize % biotic cover (e.g., macroalgal, live coral, sponge, octocoral), habitat composition, and explanatory variables for the habitat metrics (Table 3b), the orthomosaics from the SfM data were exported at ~1mm^2 resolution using the same x-y limits as the DEMs. Orthomosaics were segmented into 3m x 3m chips using MATLAB v2019a to quantify coral assemblages with an emphasis on coral morphology. Chips were imported into the MATLAB Image Labeler application to select regions of interest (ROI) using pixel and rectangle labels. Pixel labels were used for live corals and large macroalgal mats on sand to calculate the percent of abiotic and biotic cover within the survey area.

Classification of coral morphologies were based on colony size and growth trait from related studies (Zawada et al. 2019) as follows: A) submissive boulder (e.g., *Siderastrea spp*., *M. cavernosa*, *Orbicella spp*.); B) encrusting dome (e.g., *Porites astreoides*, *C. natans, D. labrinthiformis, Pseudodiploria clivosa*); C) branching (e.g., *Acropora spp.*, *Porites spp*.); D) encrusting zoanthid (*Palythoa caribaeorum*); and E) sponges (e.g., *Callyspongia plicifera, Xestospongia muta*). Reef rubble generally occurred within sandy grooves of the spur-and-groove systems, and were best labeled as pixelated areas. Soft corals such as sea fans, sea plumes and other octocorals were often moving during photography due to wave action, and were and too distorted to accurately assign pixel labels, and subsequently labeled as Rectangle ROIs.

Statistical Analyses RVC data – Potential differences in mean habitat characteristics among sites for each grouped sampling period (e.g., before vs after Irma) were tested using multivariate analyses of variance (MANOVA) models. When necessary, arcsine-square root transformation were applied to the RVC data percent cover estimates to meet assumptions of normality and homogeneity of variances prior to analysis. Canonical discriminate analysis (CDA) was used to

observe variation in the benthic community composition among sites. The scalar component or eigenvalues of each combination of habitat response variables were plotted as vectors in two-dimensional space. The direction and length of each vector identifies which habitat variables contributes significantly to the separation of site group means. Post-hoc tests included one-way analysis of variance (ANOVA) models and pairwise multiple comparisons tests (95% confidence level).

Statistical Analyses SfM habitat data – Given that each site was mapped with photogrammetry once due to the labor-intensive nature of this approach, results were summarized within each of the 3 x 3 m labeled tiles which span the spur and grove areas of the reef. Results are expressed as the percent cover of each trait-based coral group and associated habitat cover (e.g., sponge, rubble, etc.) within each tile. Potential differences in mean habitat characteristics among sites post-Irma were tested with Manova models. Post-hoc tests included one-way analysis of variance (ANOVA) models and pairwise multiple comparisons tests (95% confidence level).

Results

Protected reefs sites generally had higher mean coral cover than fished sites, but differed in dominant corals contributing to their overall structural complexity. In contrast, fished sites were more characterized by physical structures related to hardbottom habitat (e.g., vertical relief, % rubble, rugosity). Despite the hurricane impacts, RVC surveys did not show a drastic change in site characteristics and consistently described sample sites as contiguous spur-and-groove or a matrix of patchy hardbottom structures with reef rubble. The subset of sites surveyed using SfM photogrammetry (Fig. 2) provided evidence for more site-specific characteristics on within-reef complexity related to coral composition, local abiotic footprint, and small-scale variations in benthic features.

RVC Survey Results Before & After Irma – There were small variations in habitat structure and coral assemblages among sites before and after hurricane Irma; however, Manova site characterizations generally showed patterns in trade-offs between biotic cover and physical structures across both sampling eras. Before hurricane Irma, sites varied on drivers in structural features such as *a-rubble, a-hard,* and *s-hard* which grouped sites SDK, N1M, and NFS closely together (Fig. 3A), and separated these sites from those with presumably higher abundances of biotic cover (*b-coral*) such as LKP, LKU, and ESB (Figure 3B). Additionally, characterization of LKP was largely driven by and the presence of large barrel sponges (*b-sponge*) differing from LKU which was also characterized by biotic coral cover, but was also driven by metrics related to octocoral the abundance (e.g., *v-soft, b-octo*) . WSB appeared to be the only site largely driven by macroalgal cover (*b-algae*) (Fig. 3A). Anova post-hoc tests identified significant differences in depth ($p<0.01$), surface hard relief ($p=0.05$) rubble ($p=0.03$) (Table 4A). Despite the large separation between distinct spur-and-groove sites NFS and LKP, their variation in depth was not significantly different, and multiple comparisons test only identified a significant difference in rubble ($p=0.02$). Multiple comparison tests also showed LKU depth was significantly different from WDR ($p=0.03$), ESB ($p=0.03$), and WSB ($p=0.02$). Although live coral cover was not a significant driver in site characterization due to high variations in % cover for all sites, LKP and LKU exhibited the highest median % coral cover.

After the hurricane, separations among sites were largely diminished, but LKP and LKU still displayed the largest separation from other survey sites. Manova results identified *b-coral* and *a-sand* as strong variables in distinguishing among sites and showed a small inverse response in the direction of separation for sites. Additionally, the discriminant analysis reveals a separation between deeper sites with physical traits that contribute to spur-and-groove structures (e.g., *a-sand, v-hard*, *b-coral*) and shallow sites characterized by other non-coral biotic variables such as the presence of octocorals or macroalgae along the first canonical variable (Fig. 3C). Despite macroalgal cover remaining the strongest variable in characterizing WSB, sites that were previously more distant (WDR, SDK) were relatively clustered closer together after the hurricane. Post-hoc ANOVA results identified significant differences in depth ($p<0.01$), vertical hard relief ($p=0.02$), and abiotic hardbottom ($p<0.01$) (Table 4b). Less variation in diver mean depths separated sites into two groups in the multiple comparison's test where LKP's mean depth was significantly different from all sites except N1M ($p=0.07$) and NFS ($p=0.33$), while WSB was significantly different than LKP ($p<0.01$), NFS ($p=0.03$), and LKU ($p=0.02$). Additionally, multiple comparisons test identified significant differences in LKU's vertical hard relief compared to deeper sites WDR ($p=0.04$) and SDK ($p=0.05$) as well as being significantly different from all sites abiotic hardbottom except SDK ($p=0.4$) and LKP ($p=0.27$).

DEM Topographic Results – The DEM metrics captured more fine-scale habitats metrics and highlighted the influence of within site variation in benthic terrain contributing to separations among sites. For example, the SAPA (*btm_sapa*), which evaluates rugosity across neighboring cells within a site, was the most influential metric separating sites, followed by vector terrain ruggedness (*btm_vrm*) (Fig 4A). However, the general strength and direction of these metrics reveals varying levels of structural complexity along the first canonical axis. For example, RVC metrics related to physical structures (*a-hard, depth, s-hard*) generally clustered LKP and NFS as sites with physical complexity and the DEM MANOVA results also clustered these two sites (Fig. 4B) based on *btm_sapa* and *rms_roughness*. The second canonical axis separated sites based on metrics related to coral cover such as *d_crrug* in which coral dominated sites were on the lower axis. WSB was the only site not grouped with other sites because of the site's low structural complexity and higher coral cover. Post-hoc ANOVA results showed in all DEM habitat metrics being significantly different among sites except for *rms_roughness* ($p=0.21$) and relief (p=0.22) (Table 5). WSB yielded the highest median coral reef rugosity index of 3.23, and reflected a relatively shallow site (~4.3m in depth) with small variations in surface relief (2.5m) demonstrated in the depth-transect map profiles (Fig. 5C). In contrast, NFS and LKP were grouped together due to being slightly deeper sites, 6.7m and 7.3m respectively, and showed more variation in relief due to their distinct spur-and-groove formations (Fig. 5B and Fig. 5E respectively). ESB and SDK were also closely grouped together in MANOVA clustering and were not significantly different across any DEM metrics although the area analyzed using depth-transect profiles for both sites was structurally different such that SDK had several spur-and-groove formations included in analysis (Fig. 5A), while the area mapped at ESB mainly consisted of one large spur (Fig. 5D).

SfM Benthic Composition Results – Results from the orthomosaic survey displayed site variation in benthic composition, but yielded similar densities of octocorals of ~ $2/m^2$. This result is likely as static photos used in the Metashape alignment process was not able to assign tie points to moving objects such as fish or gorgonians. Canonical discriminant analysis and MANOVA

clusters showed relatively small separations among sites, but highlighted more fine-scale variations in coral assemblages and associated benthos such as encrusting zoanthids and sponges. The first canonical axis generally separated less biologically diverse sites (SDK, NFS) from sites presumably with high coral or sponge cover (LKP, ESB, WSB) (Fig. 3C). Additionally, the presence of branching corals proved to be the strongest variable in separating sites followed by sponges and encrusting dome corals. LKP and WSB were grouped together in manova clustering as these sites both demonstrated varying abundances is branching corals (Fig. 3D). For example, WSB had small patches of branching staghorn *A. cervicornis* and finger corals *Porites spp.* on , while LKP had several staghorn and elkhorn *A. palmata* coral outplants at various growth stages within the mapped area. Additionally, several brain corals were observed at LKP but had been impacted by coral disease diminishing the area characterized as live coral cover. In contrast, ESB's coral composition was dominated by mustard hill (*P. astreoides*) corals characterized as encrusting dome corals and their spatial distribution varied from patches on reef rubble to relatively denser colonies on shallow ridges. ESB also had several large boulder star coral colonies characterized as submassive corals such as the mountainous star coral *O. faveolata* and the massive starlet coral *S. siderea*.

Further distinction between coral dominated sites was dependent on the relative dominance of encrusting zoanthids and abundance of both the trait-based corals shown by post hoc ANOVA results where all fine-scale habitat metrics were significantly different ($p<0.01$) for each mapped site (Table 6). For example, although all sites were dominated by encrusting zoanthid *P. caribaeorum,* the relative percent cover was lowest at WSB (< 3.7%) and highest at NFS (< 24%) followed by LKP (< 20%) (Fig. 6G). Moreover, NFS encrusting zoanthid abundance was significantly different from all sites except previously related deeper depth site LKP ($p=0.56$). Relatively absent of encrusting zoanthids like WSB, the relative percent cove of encrusting dome corals at ESB was significantly different from all sites ($p<0.01$) (Table 6) and had the highest abundance (< 6%) (Fig. 6B). Percent cover in submassive corals at ESB was significantly different from than all sites except SDK ($p=0.99$) as both sites showed outliers greater than 5% (Table 6 and Fig. 6A respectively). Branching corals had the lowest relative percent cover out of the three coral morphologies (Fig. 6C). Multiple comparison tests identified two significant groups separating NFS from LKP ($p<0.01$). Large barrel sponges *X.muta* were abundant in LKP driving a significant difference in sponge percent cover from all sites (Table 6D) at 4.7% (Fig. 6D). Macroalgal cover was significantly different at SDK from all sites ($p<0.01$) where percent cover was highest (<32 %), while other protected sites generally had less than 1% macroalgal cover within the mapped area (Fig. 6E). Rubble percent cover was generally higher at sites previously characterized to have distinct sand channels and ridge demonstrated by SDK having the highest rubble cover (<70%) and WSB having the lowest (3.5%) (6F).

Comparison of RVC versus SfM Methods – The combination of mapping and modeling allowed for more fine-scale variables to be derived about each habitat and demonstrates how scale and methods influences site characterization. Also, the shifts in relative dominance in presumably related abiotic (e.g., *a-rubble, a-hard, btm_logsapa*) and biotic variables (e.g., *b-coral, b-sponge, branching corals*) over the RVC sampling periods and subsampled digital data provided critical thresholds for site characterization within each cluster analysis. Demonstrated in the manova results, as the habitat variable scale increased the more complex criteria became in site separation. Although coral cover was relatively low at sites for the RVC surveys, using the SfM

mapping approach showed significant differences in dominance of coral morphologies as well as related metrics such as the coral reef rugosity index, highlighting the importance of diverse coral taxa and their relative contribution to the reef framework. RVC surveys captured site variation over time while SfM mapping was more robust in observing within site variations in surface complexity across a large spatial area and captured more localized topographical features such as local depressions, patchy coral heads, and the matrix of benthos on sand (e.g., rubble, boulder corals, macroalgal turfs). For example, RVC surveys record the % live coral cover within a relatively small spatial area, and benthic surveys were not able to differentiate between coral taxa or colony size therefore structural variables were more important in site characterization. In contrast, SfM mapping allowed for multiple spatial scale approaches in site characterization by its ability to generate DEMs solely focused on structural complexity metrics and orthomosaics to understand the underlying variations in biological factors.

Implications & Future work.
This work provides baseline, fine-scale spatial data for several spur-and -groove reef sites in the FKNMS and highlights the combined use of reef visual census surveys and SfM photogrammetry to assess the physical and biological contributions to reef structural complexity relevant to coral reef management and conservation. Depth and subsurface hard relief coverage were key habitat metrics separating all sites over space and time based on both survey methods. Habitat characteristics of sites generated from RVC surveys were more closely related among sites after hurricane Irma than before. This observation is likely due to the physical impacts on the reefs such as the unearthed, cemented rubble from past disturbances, newly dislodged coral fragments, suspended sediments, and an overall decline in live coral cover at all sites for the sampling months following the hurricane. Additionally in 2017, the stony coral tissue loss disease (SCTLD) had traveled south along the Upper and Middle Keys prior to the hurricane (Muller et al. 2020) and was sighted impacting brain corals at LKP in this study's visual surveys and photogrammetry mapping in 2018.

As hard surfaces essentially include living and non-living corals, our SfM habitat mapping at a high resolution supports previously identified connections between structural complexity and variations in coral assemblages on coral reefs (Darling et al. 2012, 2017; Alvarez-Filip et al. 2013). High relief fished sites such as WDR, NFS, N1M and the protected site SDK were physically complex, but lacked the biological cover present at neighboring protected sites. In contrast, ESB, WSB, LKP, and LKU were unique in having higher % live coral cover than other study sites. Despite the structural differences between Looe Key and the Sambos, our results from habitat mapping and RVC surveys suggest that these protected reef sites generally have more reef-building corals than fished sites, but were also unique in their physical features (i.e., slope, hard vertical relief) and dominant coral assemblages.

Collectively, these observations help elucidate the spatial differences in marine reserve sites in addition to the importance of structural complexity, diversity in coral morphologies, and the influence of protection status over space and time in the Lower Florida Keys. This work is nearly ready for journal submission

Tables and Figures.

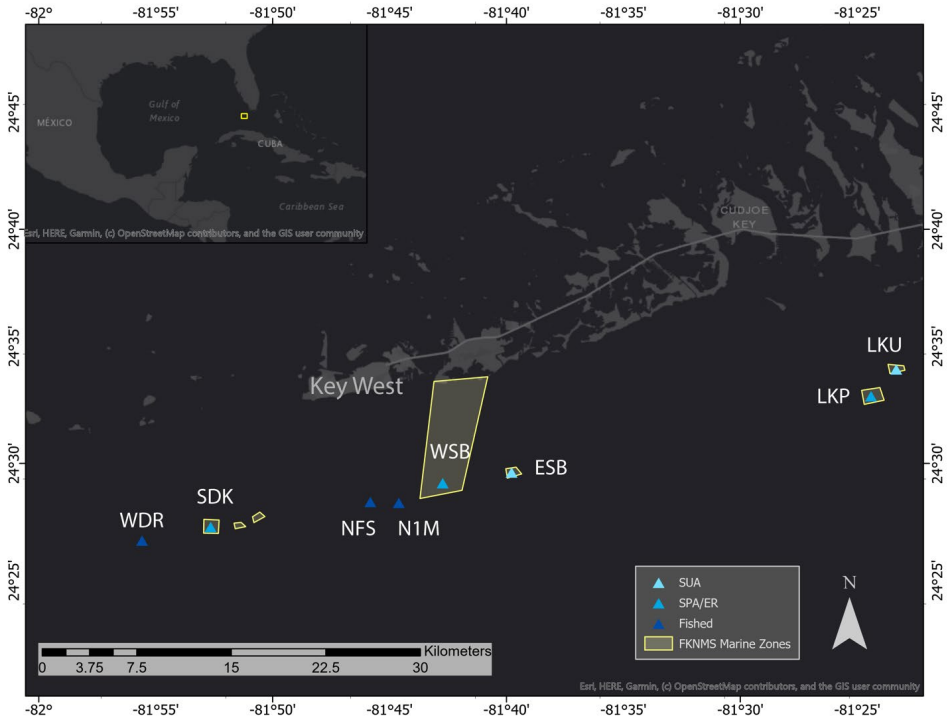

Figure 1. Study site map of zone D in the FKNMS and survey sites Western Dry Rocks (WDR), Sand Key SPA (SDK), Nine Foot Stake (NFS), Number 1 Marker (N1M), Western Sambo ER SPA (WSB), Eastern Sambo SUA (ESB), Looe Key SPA (LKP), and Looe Key SUA (LKU).

Table 1. Summary of the number of RVC and structure-from-motion (SfM) photogrammetry surveys conducted at each site between 2017 and 2018. Post-Irma surveys were conducted starting in December 2018. SfM models that were not successful in the AgiSoft Metashape reconstruction workflow are denotated (*). Not samples = NS.

	RVC									
Site	**Feb-17**	**May-17**	**Jul-17**	**Dec-17**	**Feb-18**	**Jun-18**	**Sep-18**	**Dec-18**	**Total**	**SfM Sep-18**
Fished	**2**	**3**	**3**	**3**	**1**	**3**	**2**	**2**	**19**	**2**
N1M		1	1	1		1			4	NS
NFS	1	1	1	1		1	1	1	7	1
WDR	1	1	1	1	1	1	1	1	8	*
SPA	**1**	**3**	**3**	**2**	**1**	**3**	**3**	**3**	**19**	**3**
LKP		1	1		1	1	1	1	6	1
SDK		1	1	1		1	1	1	6	1
WSB	1	1	1	1		1	1	1	7	1
SUA	**1**	**2**	**2**	**2**	**1**	**2**	**2**	**2**	**14**	**1**
ESB	1	1	1	1		1	1	1	7	1
LKU		1	1	1	1	1	1	1	7	*
Grand Total	**4**	**8**	**8**	**7**	**3**	**8**	**7**	**7**	**52**	**5**

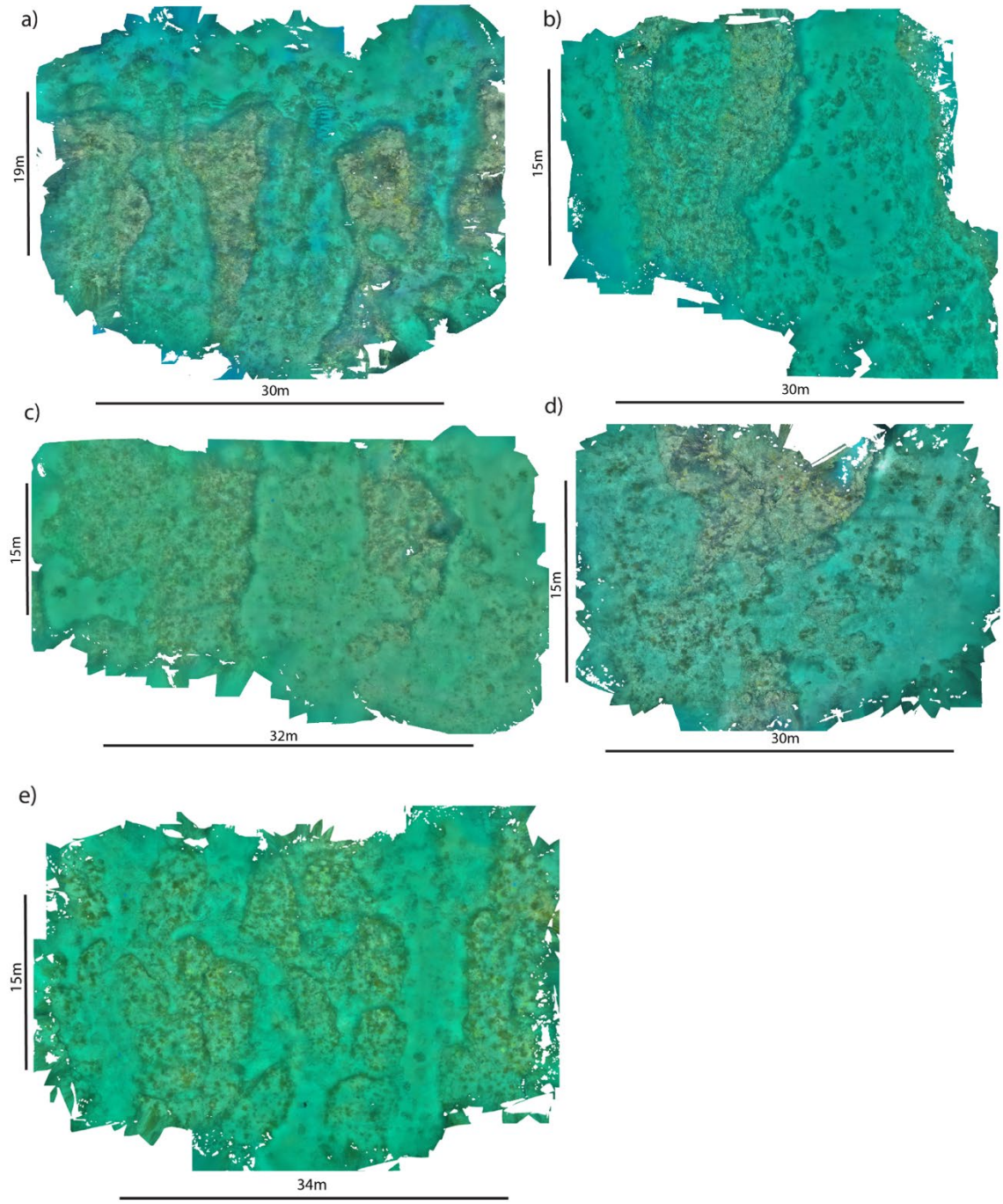

Figure 2. Summary of SfM orthomosaics created in Agisoft Metashape for SDK (A), NFS (B), WSB (C), ESB (D), and LKP (E). The scale bars represent the x and y diver-based distances between ground control points. See Table 4 for summary x-y-z (m) distances.

Table 2. Summary of digital elevation model x-y-z (m) distances, estimated square area surveyed for each site, and depth statistics (standard deviation, median, and min/max) derived from

Agisoft Metashape and ArcGIS Pro.

Site	x-dist (m)	y-dist (m)	Estimated Sq. Area (m^2)	Mean Depth (m)	SD (m)	Median (m)	Min-Max (m)
Sand Key (SPA)	30	19	570	5.3	0.90	5.4	1.9 – 7.1
Nine Foot Stake	30	15	450	6.7	0.77	7.0	3.8 – 7.7
Western Sambo (ER)	32	15	480	4.3	0.62	4.4	2.0 – 5.8
Eastern Sambo (SUA)	30	15	450	5.1	0.81	5.2	1.7 – 6.4
Looe Key (SPA)	34	15	510	7.3	0.75	7.4	4.3 – 8.9

Table 3a. Summary and descriptions of RVC habitat variables collected Pre-Irma and Post-Irma 2017-18. N=4 for both Pre- and Post-Irma.

Group	Habitat metric	Description	Variable Name
Environmental Data	Mean max depth (m)	max diver survey depth	**Max_depth**
	Visibility (m)	Diver horizontal visibility at depth	**Max_viz**
Structural Complexity	Mean max hard vertical relief (m)	max vertical relief of hard structures (e.g., coral, coralline spur, hardbottom ledge)	**Max_v-hard**
	Mean max soft vertical relief (m)	max vertical relief of soft structures (e.g., octocorals, sponges, macroalgae)	**Max_v-soft**
Surface Relief Cover	Mean % cover of hard vertical relief	estimated % hard structures within (meters): <0.2, 0.2-0.5, 0.5-1.0, 1.0-1.5, and >1.5	**Max_s-hard**
	Mean % cover soft vertical relief	estimated % soft structures within (meters): <0.2, 0.2-0.5, 0.5-1.0, 1.0-1.5, and >1.6	**Max_s-soft**
Abiotic Footprint	abiotic sand	mean % cover of coarse or biogenic sand at depth	**a-sand**
	abiotic rubble	Mean % cover of coarse gravel to unconsolidated rock or dislodged coral fragments	**a-rubble**
	abiotic hardbottom	Mean % consolidated lithogenic/biogenic substratum including dead coral	**a-hard**
Biotic Cover	biotic algae <1cm	Mean % of hardbottom covered in algae <1cm height (e.g., turf algae)	**b-algae1**
	biotic algae >1cm	Mean % of hardbottom covered in algae >1cm height (e.g., Halimeda, Dictyota)	**b-algae2**
	biotic live coral	Mean % of live coral cover	**b-coral**
	biotic octocoral	Mean % of octocoral cover	**b-octo**
	biotic sponge	Mean % of sponge cover	**b-sponge**

Table 3b. Summary and descriptions of photogrammetry habitat variables collected for benthic composition analysis. Software and toolbox/license for ArcMap and MATLAB are also listed.

Group	Habitat metric	Description	Software/License	Variable Name
Habitat complexity – Digital Elevation Model (0.5mm res)	Mean depth (m)	DEM depth	ArcMap	**btm depth**
	Mean slope	maximum change in z-values of each 3x3 cell neighborhood	ArcMap/Spatial Analyst	**btm logslope**
	Mean vector terrain ruggedness (VTM)	magnitude of each cell surface roughness across a 3x3 moving window; used the mean log transformed data	ArcMap/BTM	**btm vrm**
	Mean surface area to planar area ratio (SAPA)	rugosity evaluated across each 3x3 cell neighborhood	ArcMap/BTM	**btm logsapa**
	Rms roughness	Standard deviation of depth	MATLAB	**rms_rough**
	Digital relief	Range of depth along digital transects	MATLAB Mapping Toolbox	**d_relief**
	Digital coral reef rugosity index	*C=1-D/L* where *D* is the contour transect line and *L* the straight horizontal distance	MATLAB	**d_crrug**
Habitat Composition – Orthomosaic (1mm res)	mean hard live coral* cover, %	Mean % cover of live hard/stony corals	MATLAB Image Labeler	**Live coral**
	Mean % sponge cover	% sponge cover	MATLAB Image Labeler	**sponge**
	Mean % macroalgal cover	% macroalgal turfs on the sandy bottom/grooves	MATLAB Image Labeler	**macroalgae**
	mean % rubble cover	% coarse gravel to unconsolidated rock or dislodged coral fragments	MATLAB Image Labeler	**rubble**
	Mean density of octocorals	Density of octocorals per sq.m area mapped	MATLAB Image Labeler	**Den-octo**
	Mean % cover encrusting Zoanthid	encrusting zoanthid *Palythoa caribaeorum*	MATLAB Image Labeler	**zoan**
Trait-Based Coral Groups*	submassive	Starlet Coral (*Siderastera sidera, S. radians*), Star Coral (*Montastrea cavernosa, Orbicella annularis, O.faveolata, O. frankski*)	MATLAB Image Labeler	**submasive**
	encrusting dome*	Mustard Hill Coral (*Porites astreoides*), Brain Coral (*Colpophyllia*	MATLAB Image Labeler	**encdome**

branching*	*natans, Pseudodiploria. clivosa, Diploria labrinthifomis*) Staghorn Coral (*Acropora cervicornis, A. palmata*), Finger Coral (*Porites porites*), Yellow pencil coral (*Madracis auretenra*)	MATLAB Image Labeler	**branch**

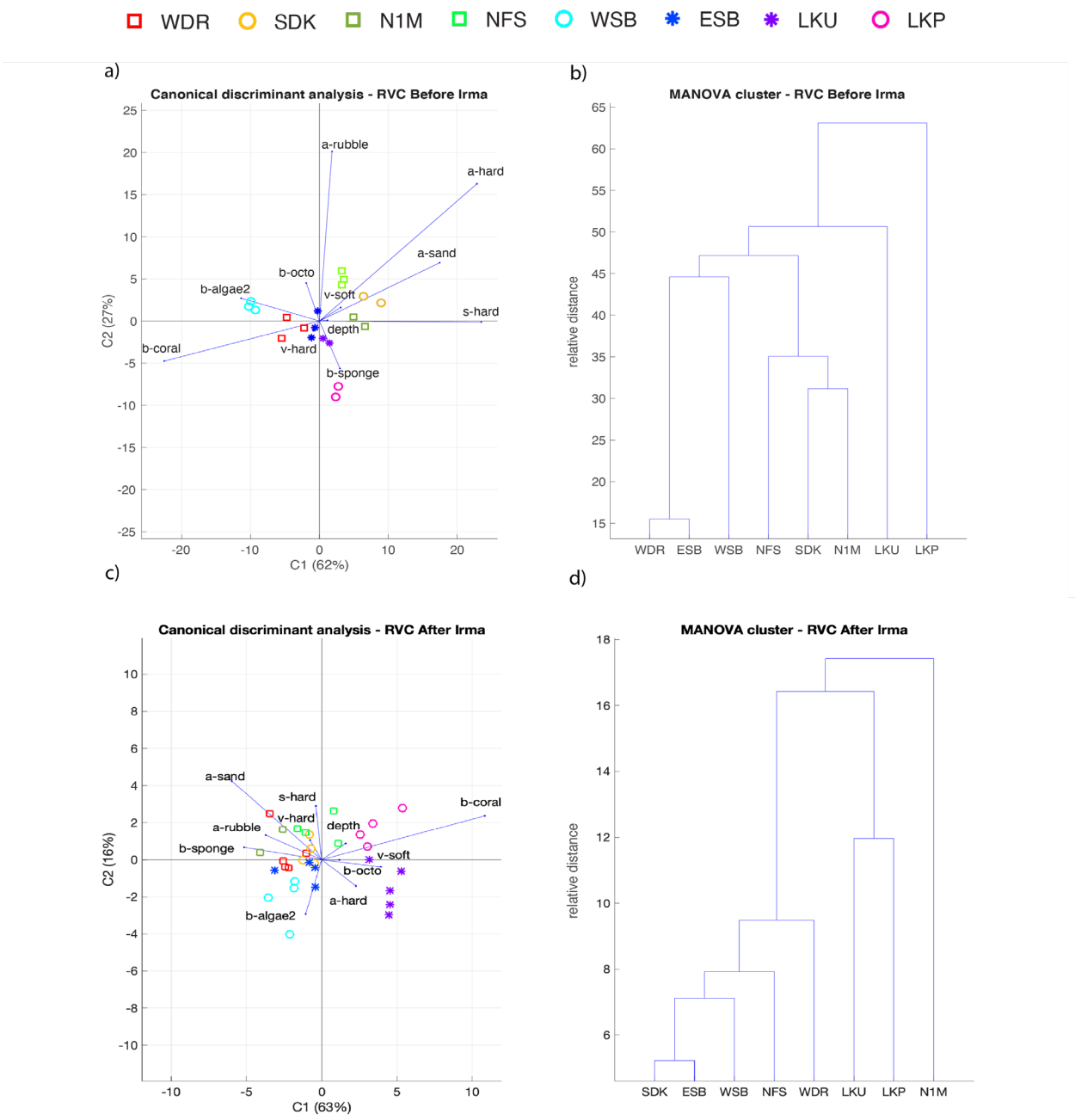

Figure 3. Canonical discriminant analyses (left) and Manova-based clusters (right) for RVC data before Irma (A, B) and RVC data after. See Table 2a for data source and habitat variable definitions.

Table 4. ANOVA results for RVC surveys before (A) and after (B) Hurricane Irma.

RVC1				
'Source'	**'df'**	**Source'**	**'F'**	**'Prob>F'**
'Groups'	7	depth	6.05	<0.01
'Error'	12	v-hard relief	0.94	0.51
'Total'	19	v-soft relief	0.87	0.55
		s-hard relief	2.91	0.05
		a-hardbottom	0.65	0.71
		a-rubble	3.31	0.03
		a-sand	2.09	0.13
		b-algae	1.49	0.26
		b-coral	0.79	0.61
		b-octo	2.00	0.14
		b-sponge	0.49	0.83

RVC2				
'Source'	**'df'**	**Source'**	**'F'**	**'Prob>F'**
'Groups'	7	depth	5.86	<0.01
'Error'	24	v-hard relief	3.07	0.02
'Total'	31	v-soft relief	0.85	0.56
		s-hard relief	2.06	0.09
		a-hardbottom	4.09	<0.01
		a-rubble	0.89	0.53
		a-sand	1.99	0.10
		b-algae	1.65	0.17
		b-coral	1.16	0.36
		b-octo	1.88	0.12
		b-sponge	0.92	0.51

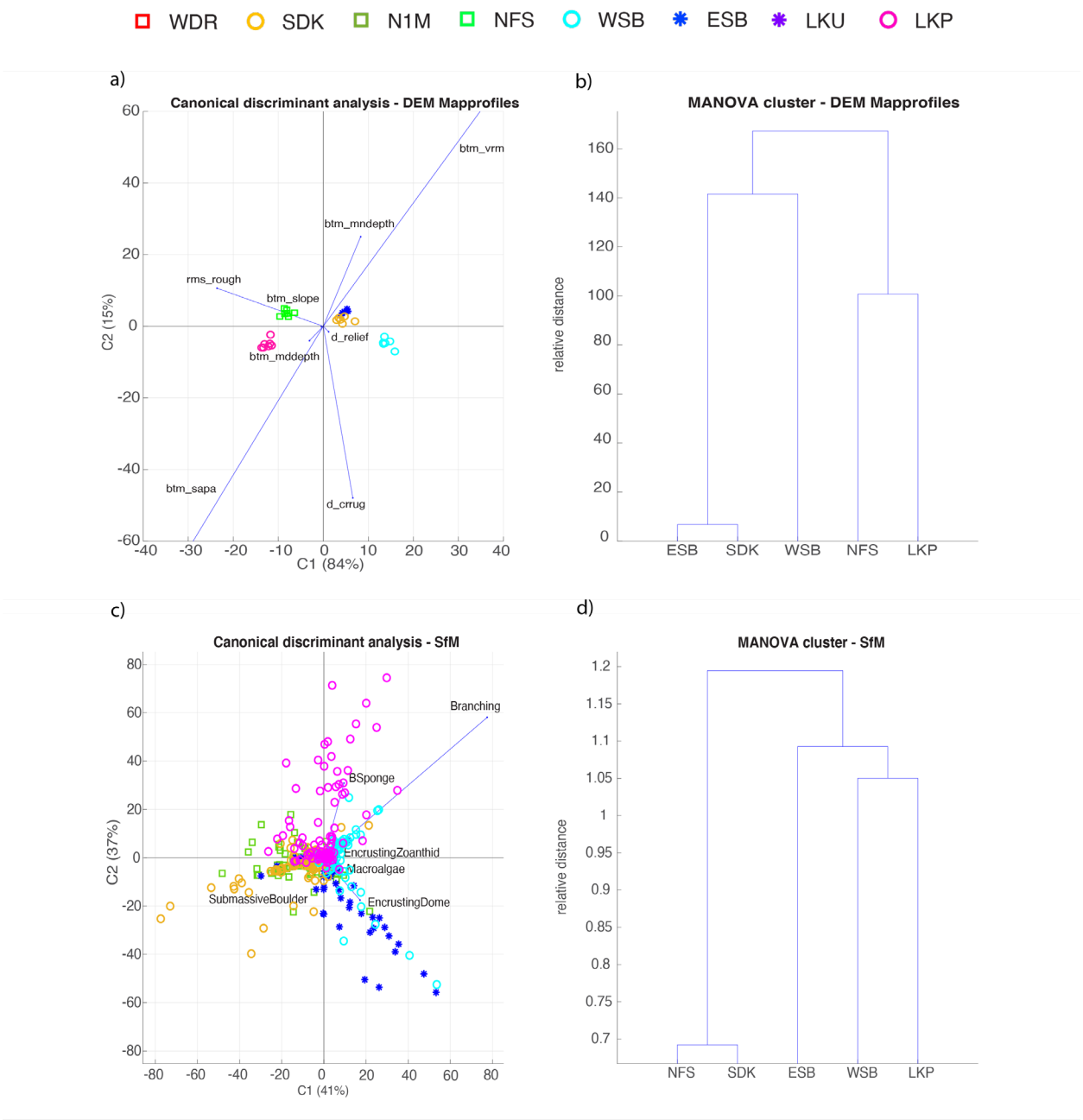

Figure 4. Canonical discriminant analyses (left) and Manova-based clusters (right) for digital elevation model (DEM) variables (A, B) and structure-from-motion (SfM) variables (C, D). See Table 2b for data source and habitat variable definitions.

Table 5. ANOVA results for DEM (A) and SfM (B) habitat variables.

DEM		**DEM**		
'Source'	**'df'**	**Source'**	**'F'**	**'Prob>F'**
'Groups'	4	mean depth	60.97	<0.01
'Error'	28	median depth	73.28	<0.01
'Total'	32	crrug	45.25	<0.01
		rms rough	1.56	0.21
		d_relief	1.53	0.22
		btm_slope	3.11	0.03
		btm_vrm	3.85	<0.01
		btm_sapa	4.56	<0.01

a)

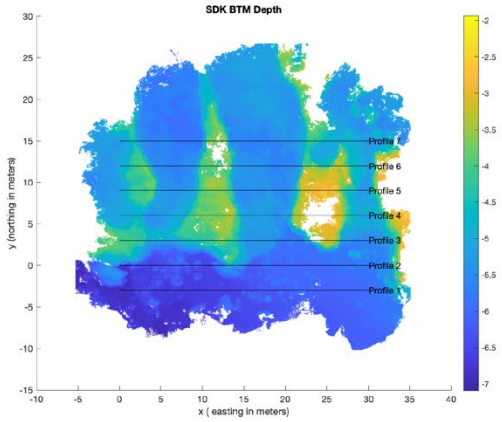
SDK BTM Depth
Profile 7
Profile 6
Profile 5
Profile 4
Profile 3
Profile 2
Profile 1
y (northing in meters)
x (easting in meters)

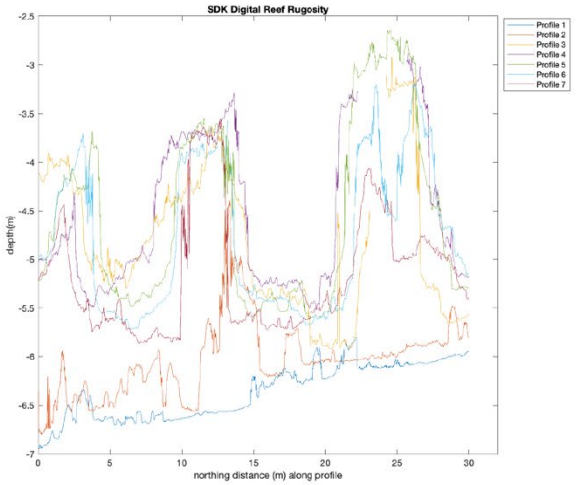
SDK Digital Reef Rugosity
Profile 1
Profile 2
Profile 3
Profile 4
Profile 5
Profile 6
Profile 7
depth(m)
northing distance (m) along profile

b)

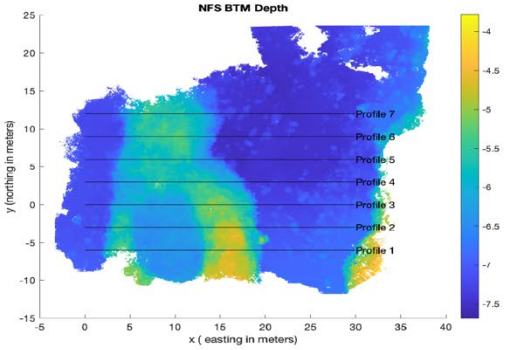
NFS BTM Depth
Profile 7
Profile 6
Profile 5
Profile 4
Profile 3
Profile 2
Profile 1
y (northing in meters)
x (easting in meters)

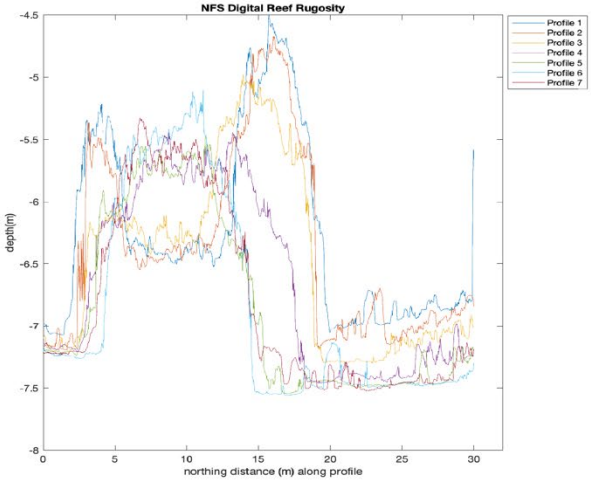
NFS Digital Reef Rugosity
Profile 1
Profile 2
Profile 3
Profile 4
Profile 5
Profile 6
Profile 7
depth(m)
northing distance (m) along profile

c)

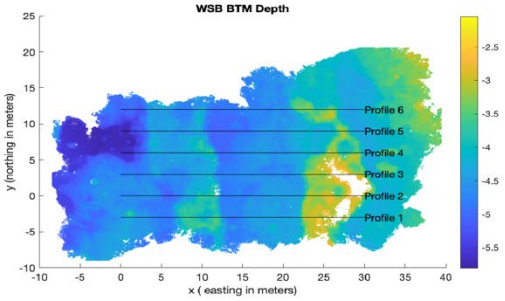
WSB BTM Depth
Profile 6
Profile 5
Profile 4
Profile 3
Profile 2
Profile 1
y (northing in meters)
x (easting in meters)

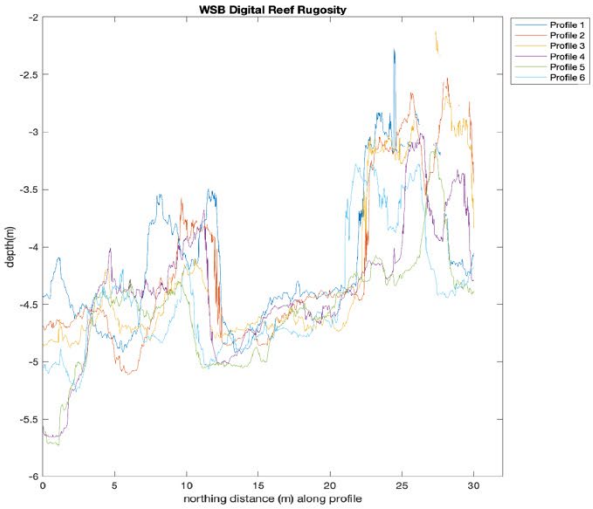
WSB Digital Reef Rugosity
Profile 1
Profile 2
Profile 3
Profile 4
Profile 5
Profile 6
depth(m)
northing distance (m) along profile

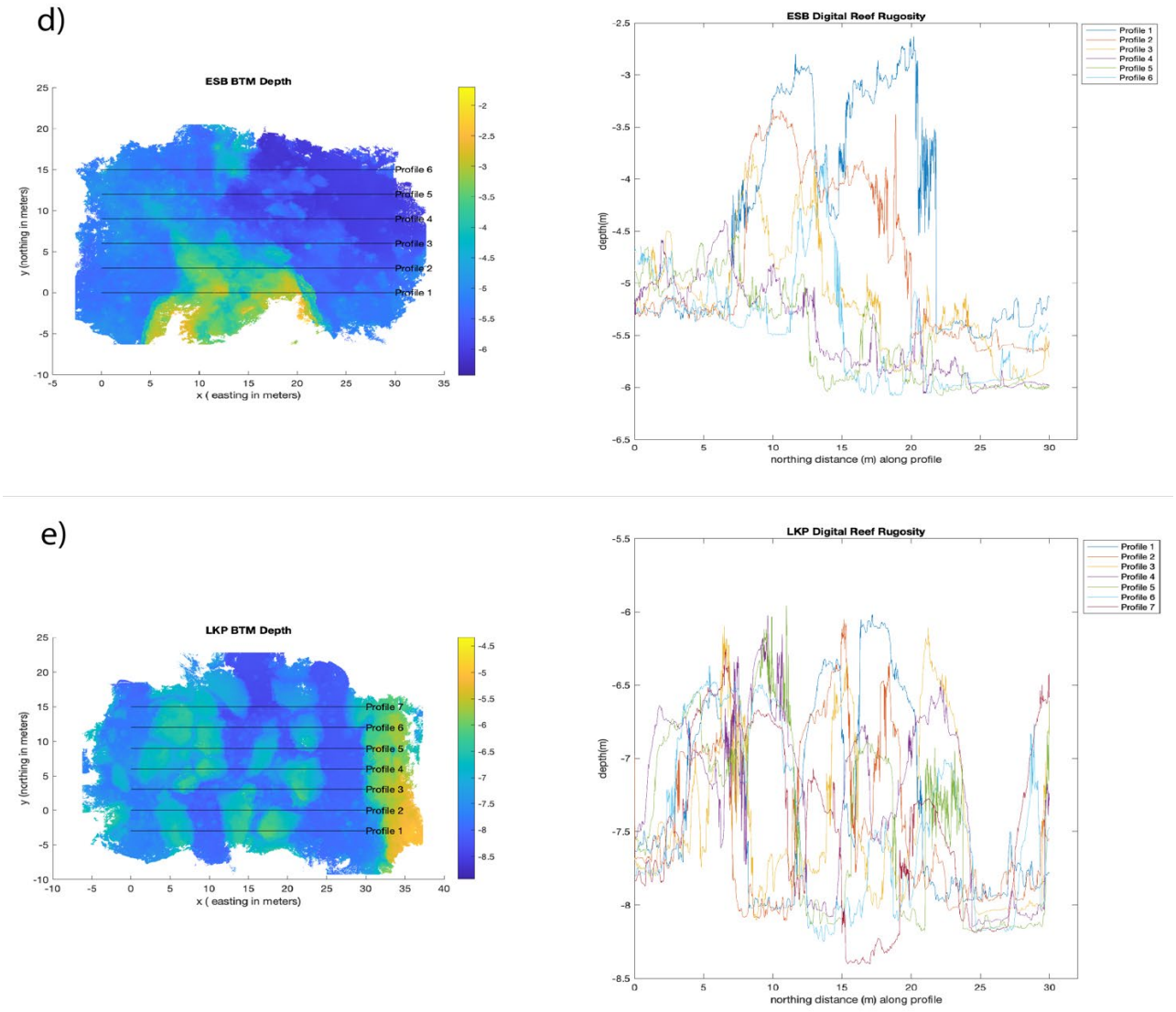

Figure 5. Scan line analysis results using MATLAB Mapping Toolbox. Depth-transect profiles (left) and digital reef rugosity (right) are shown for a) Sand Key, b) Nine Foot Stake, c) Western Sambo, d) Eastern Sambo, and e) Looe Key SPA. Transect profiles are 30m in length (west-east) with 3m spacing between transects heading in a northerly direction.

Table 6. ANOVA results for SfM habitat variables.

SfM				
'Source'	**'df'**	**Source'**	**'F'**	**'Prob>F'**
'Groups'	4	submassive boulder	6.66	<0.01
'Error'	745	encrusting dome	24.15	<0.01
'Total'	749	branching	8.32	<0.01

sponge	23.86	<0.01
macroalgae	10.53	<0.01
rubble	14.57	<0.01
encrusting zoanthid	12.64	<0.01

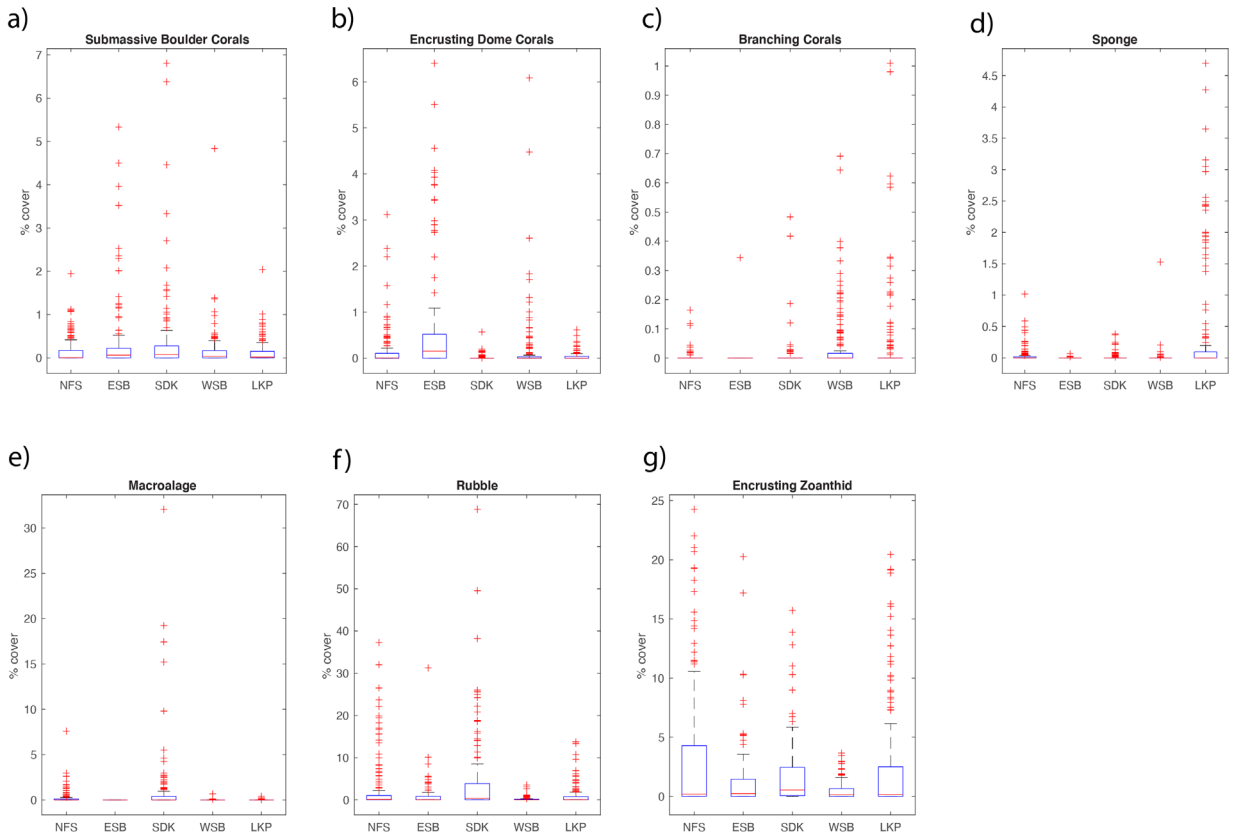

Figure 6. Box-plots of percent cover of habitat variables for five sites derived from each site's orthomosaic tiles annotated in MATLAB ImageLabeler. The central red line represents the median and the 25th and 75th percentiles are shown as the upper and lower limits respectively. Outliers are denoted as red '+' symbols.

2. Reef fish distribution, abundance and diversity - No-take marine reserves (NTMRs) were established to both decrease the exploitation of target and non-target species and rebuild depleted stocks, while protecting the integrity of biodiversity within marine ecosystems (Bohnsack & Ault 1996; Allison et al. 1998; Lubchenco et al. 2003, Ludford et al. 2012). Since first establishing NTMRs, they have produced several benefits such as increasing target fish species density, increasing spawning stock biomass, supplying source populations for neighboring habitats (i.e. spill-over), preserving trophic interactions, and protecting essential reef habitat from structural damage (Halpern 2003; Gardmark et al. 2006, Peters et al. 2017 and references therein). Generally, species diversity is increased inside marine reserves (Halpern 2003), but the variable processes that influence diversity within and around reserves still needs to be further investigated

(Sale et al. 2005). Protection from fishing can increase fish biomass, abundance, average size, and overall species diversity (Halpern 2003). In contrast, some studies indicate a decline in these biological measures or no apparent difference between fished and unfished habitats (e.g., Valles et al. 2001; Tupper & Rudd 2002).

Within one year of NTMRs being established in the FKNMS there was evidence of higher annual mean density of economically important species such as yellowtail snapper (*Ocyurus chrysurus*), grouper species (*Epinephelus sp., Mycteroperca sp*.), and hogfish (*Lachnolaimus maximus*) within NTMRs compared to fished areas; however, non-economically important species such as striped parrotfish (*Scarus iseri*) and stoplight parrotfish (*Sparisoma viride*) exhibited no uniform difference in density across fished and non-fished sites (Ault et al. 2006; Keller & Donahue 2006; Bartholomew et al. 2008). Interestingly, fish densities were generally higher in NTMRs prior to being protected in 1997 compared to fished sites (Keller & Donahue 2006), suggesting that habitat is an important explanatory variable.

For the period 1996-2002, exploited species such as gray snapper (*Lutjanus griseus*), black grouper (*Mycteroperca bonaci*), and yellowtail snapper densities were highest in NTMRs, while both striped parrotfish and stoplight parrotfish continued to show similar mean densities at fished and non-fished sites (Keller & Donahue 2006). For the period 1994-2001, changes in the relative rates of density for several important fish groups, including Haemulidae, Lutjanidae, and Serranidae were found across 22 reserve types (i.e. SPAs, SUAs, ERs) in FKNMS, and reflected an overall increased density of exploitable fishes inside reserves (Bartholomew et al. 2008). During the summer of 2003-04, transect surveys on three protected patch reef sites and two fished reference sites found that biomass and mean body lengths for several common predatory fish (i.e. *M. bonaci, E. striatus, L. griseus*) were significantly greater in the protected patch reefs than the fished patch reefs (Kramer & Heck 2007).

Methods.

Reef Visual Census (RVC) surveys followed standardized protocols developed by a cooperative multi-agency network of the Florida Fish and Wildlife Conservation Commission (FWCC), NOAA, National Park Service, and the University of Miami (Brandt et al. 2009). Primary sampling units (100 x 100m cells) within in each reef site were generated and further subdivided into a two-stage stratified random design in which two divers conducted a 15-minute reef visual census survey inside a 15m diameter cylinder. The surveys from the two divers were non-overlapping (~ 10-30 m apart), and the data from the divers were combined to produce mean values for fish density (#/m^2), whereas the number of species observed by each diver was combined.

Results.

The RVC surveys conducted during this project (Table 1) counted 14,142 individual fish and 121 species (Table 7). Mean fish densities did not vary significantly among sampling sites (1-way ANOVA, p=0.8; Figure 7a), however, mean densities did vary significantly by sampling date (1-way ANOVA, p=0.04), with mean density significantly higher in July and February 2017 compared to June 2018 (SNK multiple comparisons tests). (Figure 7b). All sites were dominated by the following fish families: Labrids, Pomacanthids, Lutjanids, with Looe Key SPA also being dominated by Haemulids, and Nine Foot Stake dominated by Scarids (Appendix Tables 1-8).

Future work. Current analyses are testing whether or not the mean density and size-frequency of target and non-target species (e.g., highlighted in Ault et al. 2006; Keller & Donahue 2006; Bartholomew et al. 2008) vary by sampling site (management zone) and season, and if these patterns generated from RVC data are consistent with species-specific sound signatures (when such signatures are known) (see Section 3 below, "Spatiotemporal variation in the underwater soundscape").

Tables and Figures.

Table 7. List of fish species observed during RVC surveys in the FKNMS (2017-18).

Scientific Name	Common Name
Abudefduf saxatilis	Sergeant Major
Abudefduf taurus	Night Sergeant
Acanthurus bahianus	Ocean Surgeonfish
Acanthurus chirurgus	Doctorfish
Acanthurus coeruleus	Blue Tang
Acanthurus tractus	Ocean Surgeonfish
Aluterus scriptus	Scrawled Filefish
Anisotremus surinamensis	Black Margate
Anisotremus virginicus	Porkfish
Apogon townsendi	Belted cardinalfish
Aulostomus maculatus	Atlantic Trumpetfish
Bodianus rufus	Spanish Hogfish
Calamus calamus	Saucereye Porgy
Cantherhines pullus	Orangespotted filefish
Canthigaster rostrata	Sharpnose Puffer
Caranx crysos	Blue Runner
Caranx latus	Horse-Eye Jack
Caranx ruber	Bar Jack
Centropomus undecimalis	Common Snook
Cephalopholis cruentata	Graysby
Chaetodipterus faber	Atlantic Spadefish
Chaetodon capistratus	Foureye Butterflyfish
Chaetodon ocellatus	Spotfin Butterflyfish
Chaetodon sedentarius	Reef Butterflyfish
Chaetodon striatus	Banded Butterflyfish
Chromis cyanea	Blue Chromis
Chromis insolata	Sunshinefish

Chromis multilineata	Brown Chromis
Chromis scotti	Purple Reefish
Clepticus parrae	Creole Wrasse
Coryphopterus glaucofraenum	Bridled goby
Dasyatis americana	Southern Stingray
Diplodus holbrookii	Spottail Pinfish
Echeneis naucrates	Live sharksucker
Echeneis neucratoides	whitefin sharksucker
Elactinus lobeli	Caribbean Neon Gobi
Elacatinus oceanops	Neon Gobi
Epinephelus adscensionis	Rock Hind
Epinephelus guttatus	Red Hind
Epinephelus morio	Red Grouper
Epinephelus striatus	Nassau Grouper
Equetus punctatus	Spotted Drum
Gramma dejongi	Golden basslet
Gramma loreto	Fairy basslet
Gerres cinereus	Yellowfin Mojara
Ginglymostoma cirratum	Nurse Shark
Gnatholepis thompsoni	Goldspot gobi
Gymnothorax funebris	Green Moray
Gymnothorax moringa	Spotted Moray
Haemulon album	White Margate
Haemulon aurolineatum	Tomtate Grunt
Haemulon carbonarium	Caeser Grunt
Haemulon chrysargyreum	Smallmouth Grunt
Haemulon flavolineatum	French Grunt
Haemulon macrostomum	Spanish Grunt
Haemulon melanurum	Cottonwick
Haemulon parra	Sailors Choice
Haemulon plumierii	White Grunt
Haemulon sciurus	Bluestriped Grunt
Halichoeres bivittatus	Slippery Dick
Halichoeres cyanocephalus	Yellowcheek Wrasse
Halichoeres garnoti	Yellowhead Wrasse
Halichoeres maculipinna	Clown Wrasse
Halichoeres poeyi	Blackear Wrasse
Halichoeres radiatus	Puddingwife

Himantura schmardae	Chupare stingray
Holacanthus ciliaris	Queen Angelfish
Holacanthus tricolor	Rock Beauty
Holocentrus adscensions	Squirrelfish
Holacentrus rufus	Longspine Squirrelfish
Kyphosus sectatrix	Bermuda Chub
Lachnolaimus maximus	Hogfish
Lactophrys triqueter	Smooth Trunkfish
Lutjanus analis	Mutton Snapper
Lutjanus apodus	Schoolmaster Snapper
Lujanus campechanus	Red Snapper
Lutjanus griseus	Gray Snapper
Lutjanus jocu	Dog Snapper
Lutjanus mahogoni	Mahogany Snapper
Lutjanus synagris	Lane Snapper
Microspathodon chrysurus	Yellowtail Damselfish
Mulloidichthys martinicus	Yellow Goatfish
Mycteroperca bonaci	Black Grouper
Mycteroperca interstitialis	Yellowmouth Grouper
Mycteroperca phenax	Scamp
Myripristis jacobus	Blackbar Soldierfish
Ocyurus chrysurus	Yellowtail Snapper
Odontoscion dentex	Reef Croaker
Panulirus argus	Spiny Lobster
Pareques acuminatus	Highhat
Pomacanthus arcuatus	Gray Angelfish
Pomacanthus paru	French Angelfish
Priacanthus arenatus	Atlantic Bigeye
Pseudupeneus maculatus	Spotted Goatfish
Pterois volitans	Red Lionfish
Sargocentron vexillarium	Dusky Squirrelfish
Scarus coelestinus	Midnight Parrotfish
Scarus coeruleus	Blue Parrotfish
Scarus guacamaia	Rainbow Parrotfish
Scarus iseri	Striped Parrotfish
Scarus taeniopterus	Princess Parrotfish
Scarus vetula	Queen Parrotfish

Scomberomorus regalis	Cero
Scorpaena plumieri	spotted scorpionfish
Seriola dumerili	Greater Amberjack
Seriola rivoliana	Almaco Jack
Serranus tabacarius	Tobaccofish
Serranus tigrinus	Harlequin Bass
Sparisoma aurofrenatum	Redband Parrotfish
Sparisoma chrysopterum	Redtail Parrotfish
Sparisoma radians	Bucktooth Parrotfish
Sparisoma rubripinne	Yellowtail Parrotfish
Sparisoma viride	Stoplight Parrotfish
Sphyraena barracuda	Great Barracuda
Stegastes adustus	Dusky Damselfish
Stegastes diencaeus	Longfin Damselfish
Stegastes leucostictus	Beaugregory
Stegastes partitus	Bicolor Damselfish
Stegastes planifrons	Three-spot Damselfish
Stegastes variabilis	Cocoa Damselfish
Thalassoma bifasciatum	Bluehead wrasse

Figure 7a. Spatial variation: Mean density (± SE) of fish counted by 2-3 divers conducting RVC surveys--data averaged among the divers at a given site and time (2017-18, see Table 1 for summary of RVC surveys).

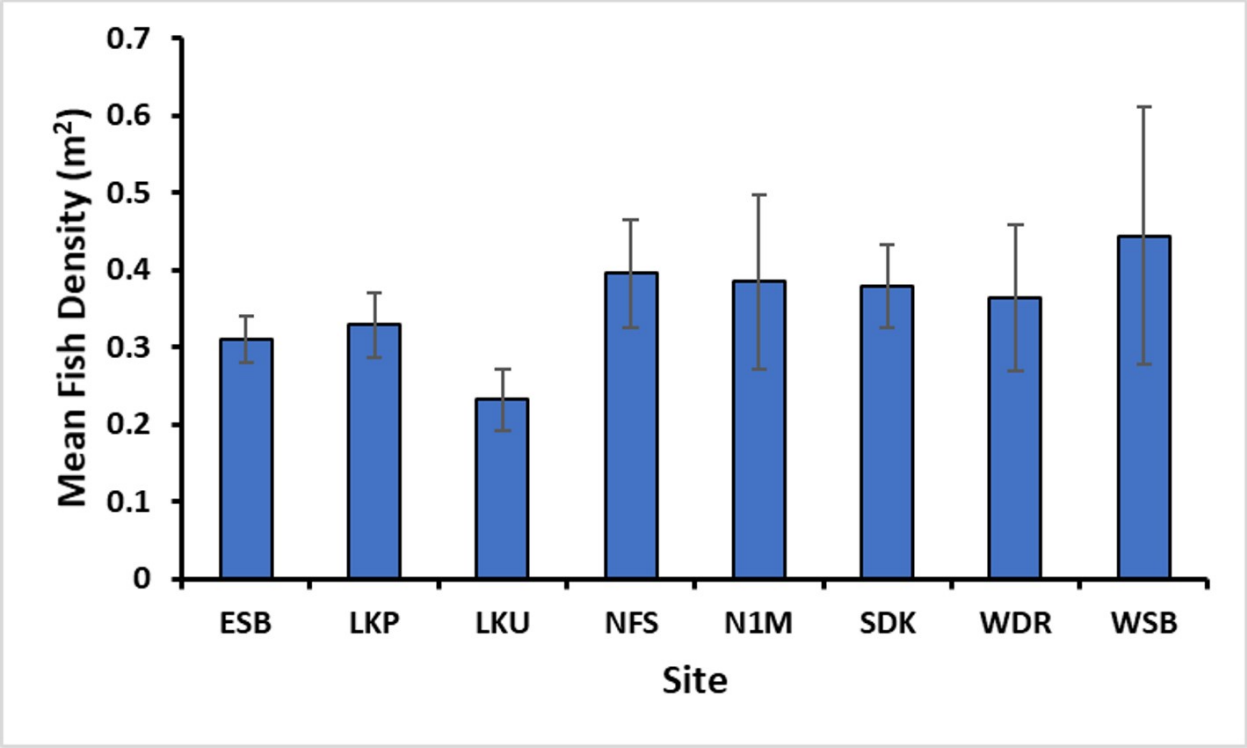

Figure 7b. Temporal variation: Mean density (± SE) of fish counted by 2-3 divers conducting RVC surveys--data averaged among the divers at a given site and among sites within a given sampling time period (2017-18, see Table 1 for summary of RVC surveys).

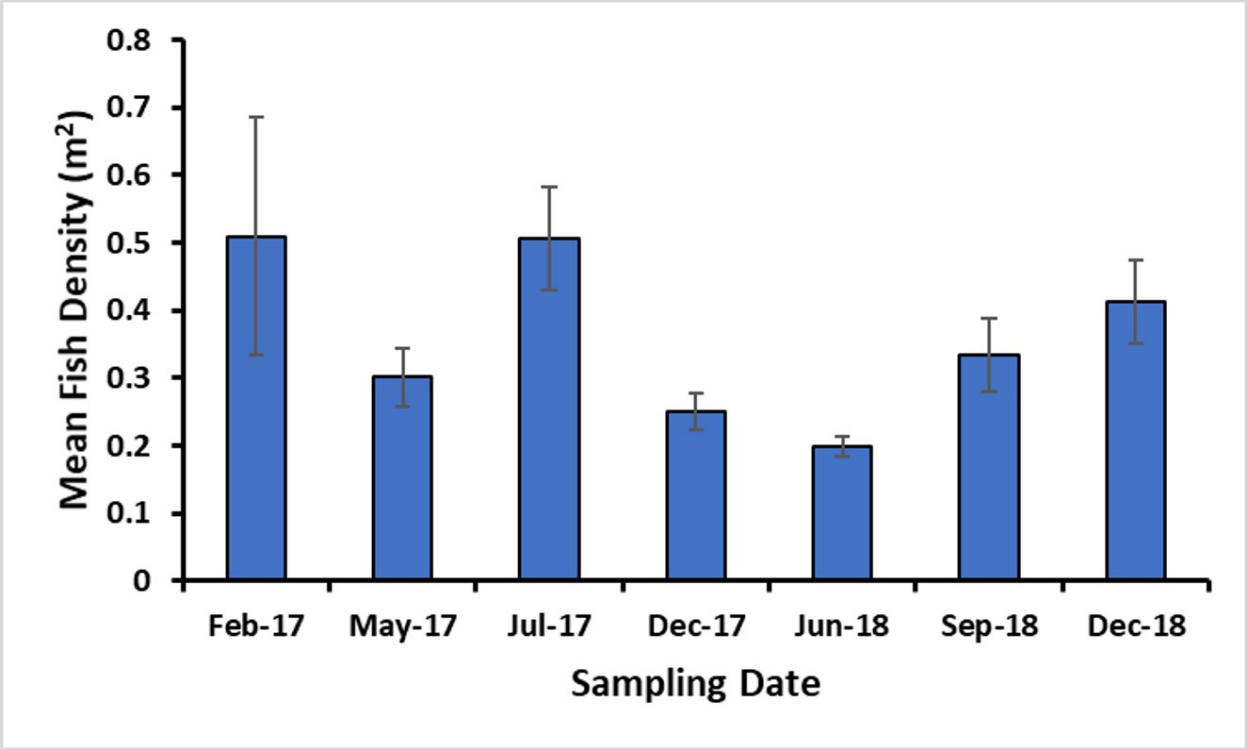

3. Spatiotemporal variation in the underwater soundscape

The local soundscape, which is a combination of physical (wind, waves, etc.), biological (calls and feeding sounds, etc.) and anthropogenic (vessels, construction, etc.) sound sources, plays an important role for many species and in numerous ecosystems (Krause 1987). The role of sound for communication by marine mammals, fish and invertebrates is documented in several recent reviews (Tidau & Briffa 2016; Lindseth & Lobel 2018; and references therein). For example, blue whales produce low-frequency calls to find mates, fish produce low-frequency choruses to communicate with and attract mates, and snapping shrimp produce broadband sounds that can stun prey and defend territories (Versluis et al. 2000; Montie et al. 2015 and references therein). Examples of communication in the marine realm are wide-ranging, and also highlight how many animals hear and respond to frequencies outside of those they produce (Slabbekoorn et al. 2010).

Generally at spawning aggregation sites, fish (usually males) produce calls to attract potential partners (Lugli et al. 1986; Myrberg et al. 1986). In the Western Atlantic and Caribbean, spawning grouper aggregations are being increasingly monitored using passive acoustic methods. Previously described Serranid sounds with verified correlation with known spawning seasons include the goliath grouper (*Epinephelus itajara*), red hind (*E. guttatus*), red grouper (*E. morio*), yellowfin grouper (*Mycteroperca venenosa*), Nassau grouper (*E. striatus*), and black grouper (*M. bonaci*) (Mann et al. 2010; Schärer et al. 2012, 2013 and references therein). For

example, red hind produced a low-frequency call with mixed tonal-pulse sounds associated with courtship and territorial behaviors during spawning aggregations (Locascio & Mann 2008; Mann et al. 2010). Red hind sound production typically displays trends reflecting male presence (Mann et al. 2010), an increase in density, and post-spawning depensation (Nemeth et al. 2007), with maximum sound pressure levels occurring at sunset during spawning activities (Mann et al. 2010). Only one study has attempted to use passive acoustics in combination with diver visual surveys to understand red hind populations (Rowell et al. 2012). In 2010-2012 at Riley's Hump located in the Tortugas South Ecological Reserve, Florida Keys, sound production from several grouper species, including the yellowfin grouper (rare), black grouper, red grouper, and red hind occurred at distinct periods during the winter-spring spawning seasons (Locascio & Burton 2016). While the frequency ranges of the calls associated with black, yellowfin and Nassau groupers overlap slightly, the duration and time-frequency structure are notably different, allowing their vocalizations to be discerned from one another (Nelson et al. 2011, Schärer et al. 2013). Identification and characterizing of spawning aggregations is critical to understanding life histories and conducting stock assessments. Passive acoustics is an emerging tool that can be used to identify key reproductive habitat and estimate abundances (e.g., Rowell et al., 2012). Such information can be collected semi-continuously, even at night when visual surveys are not effective, and over time scales that cannot be achieved using diver surveys or active acoustic campaigns.

Methods.

Soundscape patterns were characterized over the course of a year at six sites along a 55-km-long section of spur-and-grove, fore-reef habitat between Western Dry Rock and Looe Key reefs, within the Florida Keys National Marine Sanctuary (FKNMS). The data are summarized in terms of the sound pressure levels within both low and high frequency bands to separate components of the soundscape influenced predominantly by fish and invertebrate sound production, respectively.

Key Questions:

1. What is the nature of the soundscape within these spur-and-groove coral reef habitats?
2. How do biological inputs to the soundscape vary spatially and temporally?
3. Which sites are influenced more heavily by anthropogenic noise?

Data Sources:

1. Passive acoustic data from six sites over a period of one year.
2. Environmental data on wind speed and water temperature
3. High-resolution satellite imagery.

Methods:

Between December 2017 and December 2018, acoustic data were collected semi-continuously at six sites within the Lower Keys Region of the Florida Keys National Marine Sanctuary (FKNMS). The instrumentation captured two-minutes of acoustic data every 20 minutes at a sample rate of 48 kHz. Water temperature was recorded *in situ* during each two-minute acoustic sampling window. In addition to the Methods and Results shown below, current analyses are identifying species-specific sound signatures (call patterns), and testing whether or not the

presence of species identified via passive acoustic techniques varies across space and time in a manner consistent with related data generated from RVC surveys.

The monitoring sites include two Special Use Areas (LKU, LKP) where entry is restricted, a Sanctuary Preservation Areas (LKP) and an Ecological Reserve site (WSB) where fishing is prohibited, however, boats may moor using established buoys, and two non-regulated sites (NFS and WDR) where fishing and anchoring (on non-coral substrate) are permitted (Fig. 8).

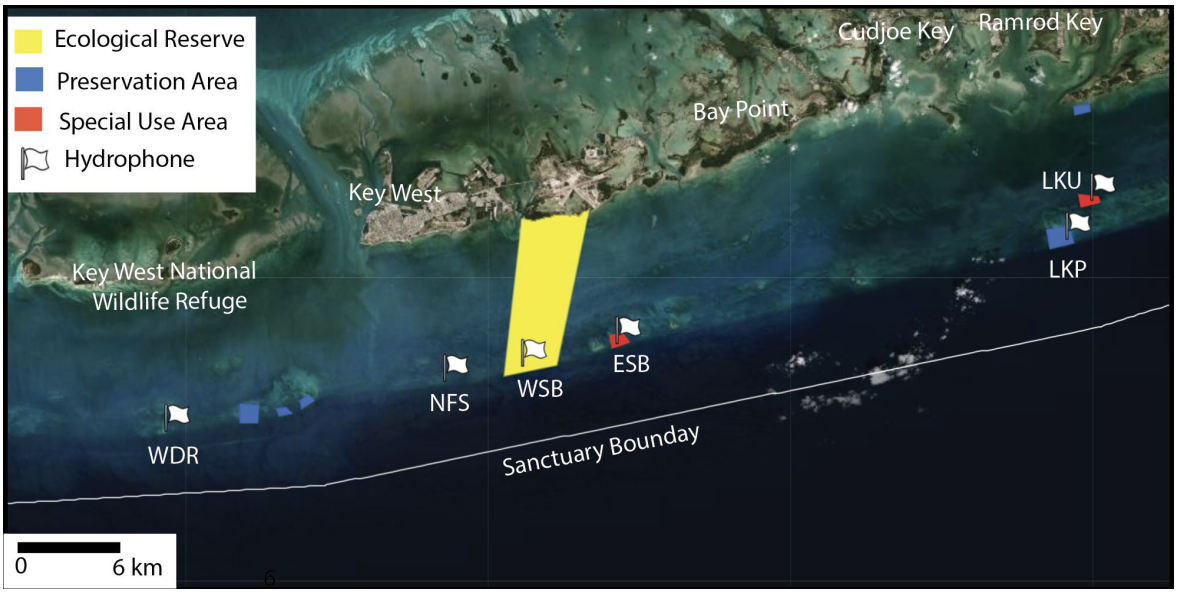

Figure 8. Map of passive acoustic monitoring locations within the Lower Keys Region of the Florida Keys National Marine Sanctuary. LKU (Looe Key - Special Use), LKP (Looe Key - Preservation Area), ESB (Eastern Sambo-Special Use Area), WSB (Western Sambo - Ecological Reserve), NFS (Nine-Foot Stake), and WDR (Western Dry Rock).

The hydrophones were attached to a weighted frame at a height of 0.15 m above the seabed, and in water depths of ~5 m. Each instrument was similarly positioned within the spur (corals) and groove (sand or hard bottom) substrates that characterize these fore-reef areas (e.g., Figure 9). These terrains provide valuable structural habitat, with 2-3 m of local relief, and can serve as popular recreational sites for diving, snorkeling and fishing within the Lower Keys Region (Fig. 8).

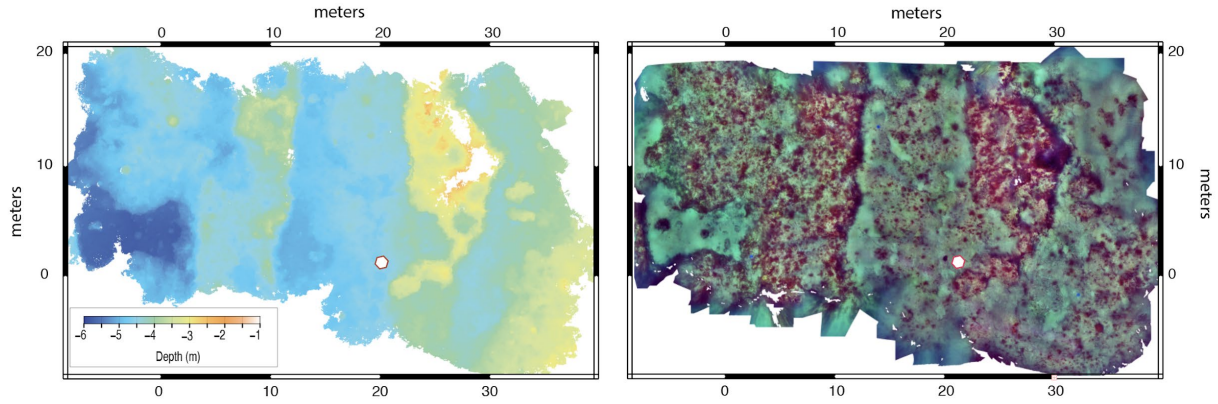

Figure 9. Fine scale bathymetry and orthomosaic image of the seafloor within the Western Sambo (WSB) reef. The white dot denotes the location of the hydrophone. This spur-and-groove morphology is typical of the habitats monitored in this study. These high-resolution maps were created using 1000's of photographs taken by a diver swimming back and forth across the reef.

Wind speeds and directions averaged over six minute intervals were obtained from the NOAA Water Level Observation Network station in Key West Florida. Water temperatures measured by the recorders were highly correlated across the Lower Keys Region, and therefore averaged to provide a single time series (Fig. 10).

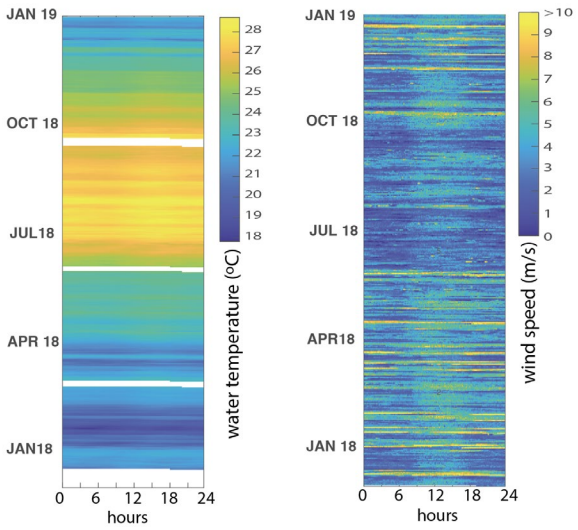

Figure 10. (a) Average water temperature from *in situ* sensors across the six monitoring sites in the Lower Keys, sampled every 20 minutes, and (b) wind speed data from a NOAA monitoring site at Key West Florida.

The raw acoustic data were corrected to pressure (**µ**Pa) using instrument specific calibrations. Since our interest is in the ambient sound pressure levels (SPLs), we analyze the 60-sec segment of data within each recording with the smallest root-mean-squared amplitude. This approach is effective at excluding high amplitude transient signals caused by the physical interaction of animals with the hydrophone ("fish-bumps"), and acts to suppress some amount of transient boat

noise by excluding signals sourced within a vessel's closest window of approach. In the absence of these signals, this subsampling has little impact on the reported SPLs.

Sound pressure levels were calculated over different frequency bands to investigate various components of the soundscape. Here, we present a time series of sound pressure levels with a high-frequency band (5-20 kHz), where invertebrate sounds are expected to dominate, and a low frequency band (0.05-1.5 kHz), where fish vocalizations are the primary source of biophony. Acoustic data in each frequency band were organized by hour and day, forming a matrix of SPL's expressed in dB re 1 **μ**Pa (Figs. 11 & 12).

Results.

The Results are described according to two images that show the temporal evolution of sound pressure levels within low and high frequency bands as a function of hour and day (Figs. 11 & 12). These images highlight similarities and differences across the Lower Keys Region of the FKNMS, identifying signals of environmental, biological and anthropogenic origin. Figure 14 shows a sound gallery of the dominate calls identified in Figs. 11 & 12.

High-frequency SPL is well correlated across the Lower Keys Region. Daytime sound levels, however, are elevated slightly within the Looe Key Preservation Area (LKP) compared to the other reefs (Fig. 11). This reflects the heavy use of this area by recreational boaters--a pattern which is even more evident in the low frequency band, as described below. Inspection of the acoustic data shows that the high frequency soundscape is otherwise dominated by invertebrate noise--chiefly the barrage of impulse sounds associated with resident colonies of snapping shrimp, which generate cavitation around the tips of their rapidly closing claws. Snapping persists throughout the daytime and nighttime hours, with a slight increase in rate during crepuscular (dawn and dusk) periods. Over the course of the year, snapping rates and high-frequency sound levels reach their maximum levels during the late summer, as water temperatures peak throughout the region.

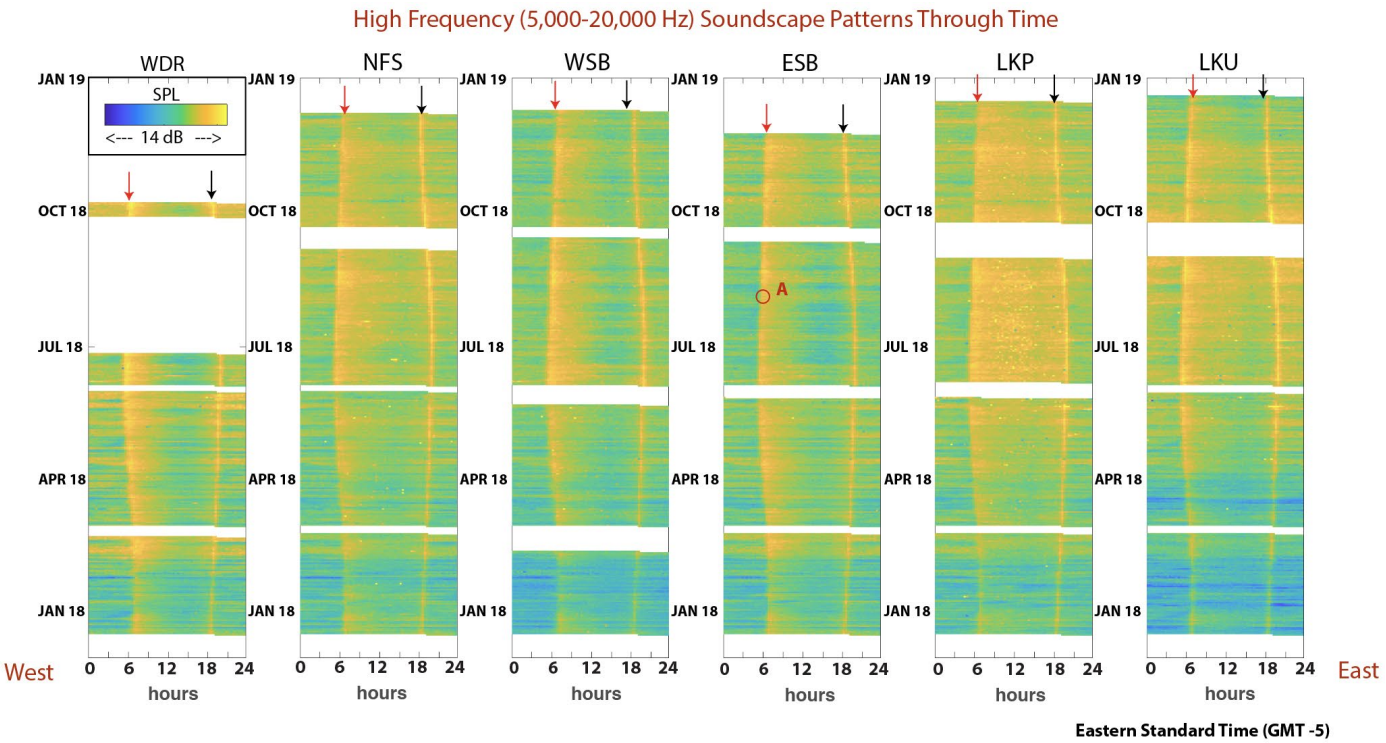

Figure 11. High-frequency SPL displayed as a function of hour and day between December 2017 and December 2018. Note the consistent diel patterns driven by an increase in invertebrate sound production during crepuscular periods, with red and black arrows showing sunrise and sunset times, respectively. The color scale is re-centered for each site to highlight temporal patterns.

At lower-frequencies (0.05-1.5 kHz), SPL is on average slightly elevated during the daytime hours relative to the night, with small crepuscular increases observed at most sites (Fig. 12). Low-frequency SPLs increase at all sites during strong wind events, yet in general SPLs are more weakly correlated between sites than observed in the higher frequency band. This divergence of the soundscape reflects differences in the local contribution of anthropogenic and biological noise.

Boat noise is evident in the low-frequency band across all sites, and dominates the daytime soundscape within the Looe Key Preservation Area (LKP), especially during the summer months. This is evident by the speckled pattern in the time series image (Fig. 12). We validate the heavy use of this site by recreational boaters using high-resolution (3m/pixel) satellite images that provide coverage of the Lower Keys Region once every few days. Figure 13 shows portions of the scene captured on Monday 13 August 2018 at 11:39 EDT, which identifies more than 17 boats positioned along the network of mooring buoys established within the Looe Key Preservation Area.

Biological inputs into the low-frequency soundscape also vary longitudinally along the Lower Keys Region. Nine-Foot Stake (NFS) is the only site where sustained nighttime vocalizations believe to be associated with the Atlantic Midshipman are observed during two distinct periods in April of 2018. Drawing on studies of the Plainfin Midship in the Pacific (e.g., Bass 1990), we

assume that males produce these harmonic sounds through contraction of their swim bladder muscles, and that these hums with fundamental frequency of ~130 Hz are used to attract females. Chorusing across the western sites, however, is more typically manifested by intermittent periods of elevated sound in the 100-500 Hz band during the daytime hours (Fig. 12 B). The species generating these calls cannot be positively identified, but notably this pattern is not readily observed at Looe Key sites (LKP, LKP) in the east. The low frequency soundscape at Looe Key is instead characterized by short bouts of nighttime calling (Fig. 12 E), and a strong chorus at dusk throughout the spring that is dominated by 'knocking' sounds (Fig. 12 F). Neither of these patterns is observed readily at the western reef sites.

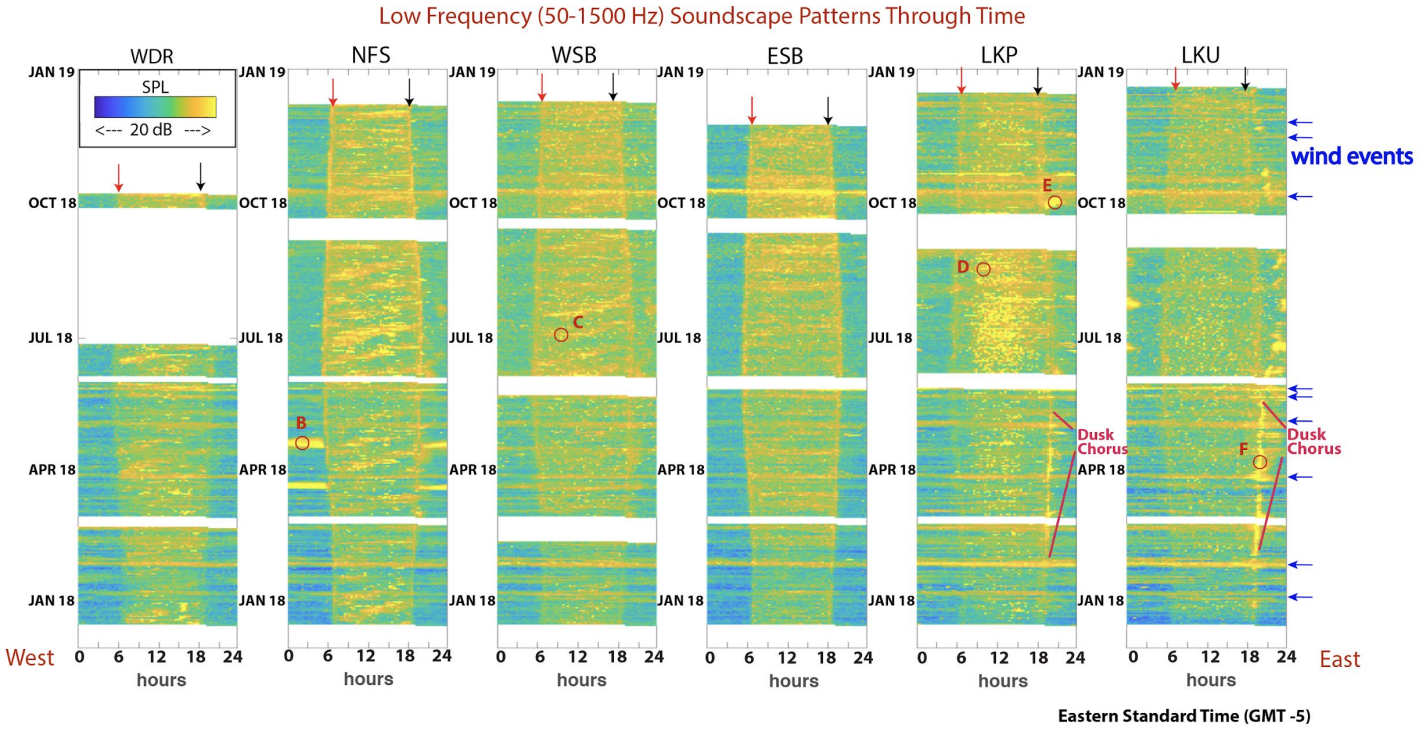

Figure 12. Low-frequency SPL displayed as a function of hour and day between December 2017 and December 2018. The letter B identifies nighttime chorusing likely associated with the Atlantic Midshipman, C marks a period of daytime chorusing in the western reefs, D period of elevated anthropogenic noise related to small recreation vessels, E marks an episode of nighttime knocking, and F shows an example of the spring-time dusk chorusing observed at both Looe Key sites. Blue arrows show episodes of low frequency noise that extend across all sites and appear to be associated with strong wind events. The color scale is re-centered for each site to highlight temporal patterns.

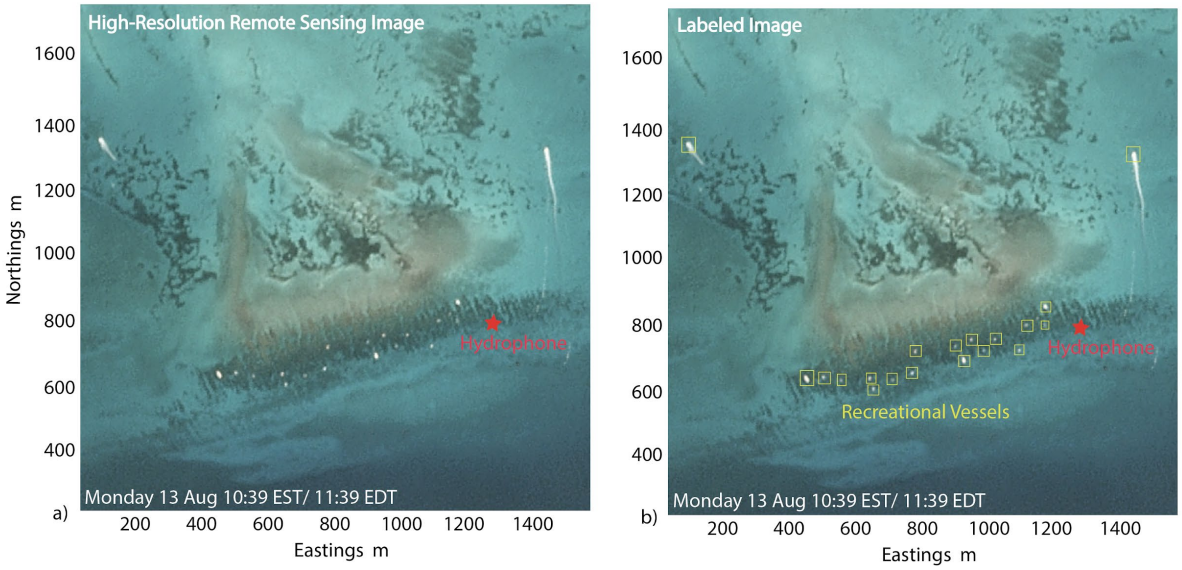

Figure 13: High-resolution red-blue-green satellite image (a) and labeled image (b) showing the location of small boats within the Looe Key Preservation Area (LKP) on Monday 13 August 2018 at 11:39 local time (EDT). This snapshot shows 17 stationary boats along the fore-reef area utilizing the network of established mooring buoys and two additional boat wakes heading away from the reef. The red star identifies the position of our hydrophone.

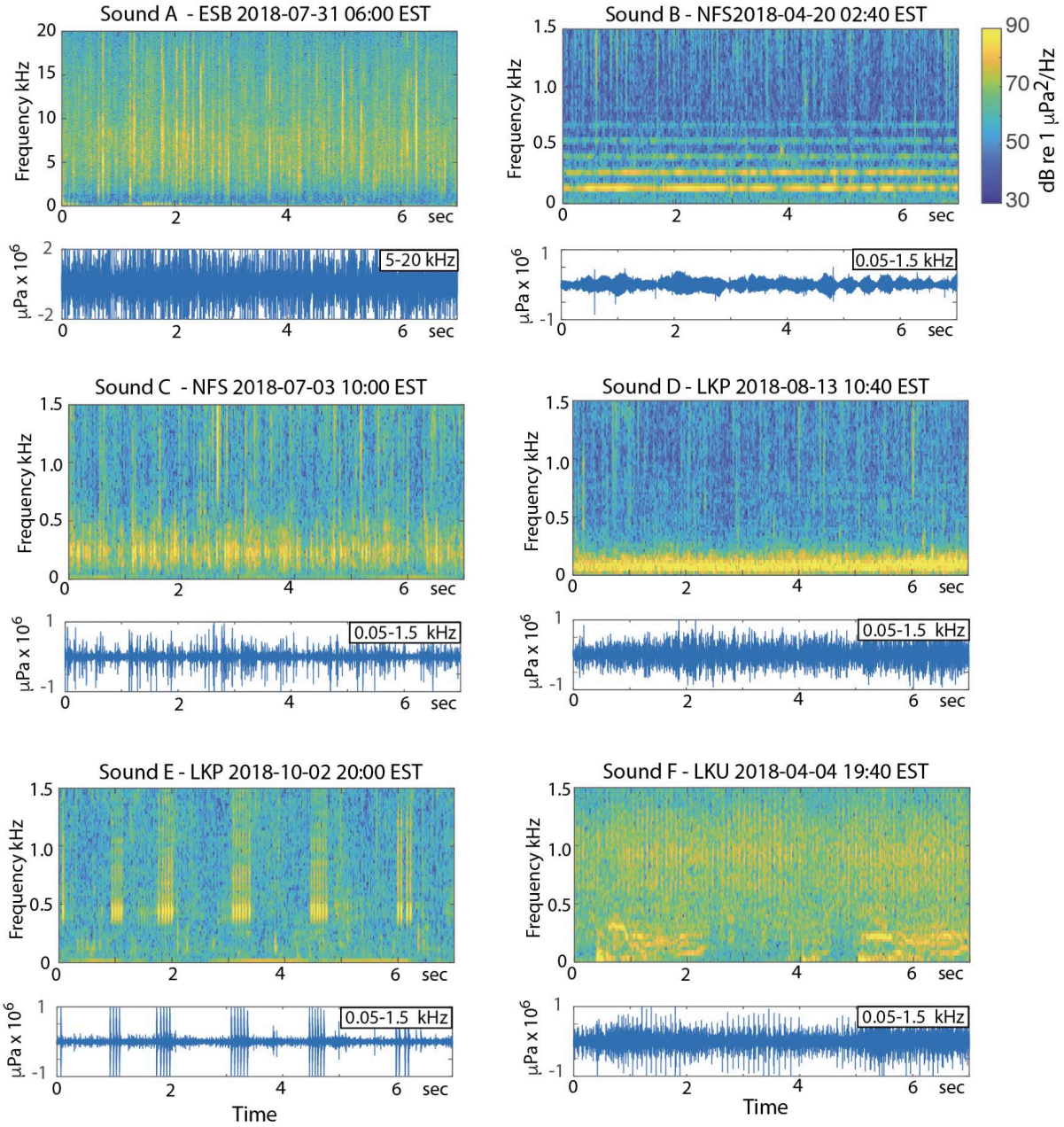

Figure 14. Lower Florida Keys sound gallery. Letters refer to chorusing episodes identified in Figs. 11 and 12. **A**) broadband impulsive signals generated by snapping shrimp; these signals dominate the high-frequency soundscape across the Lower Keys Region. **B)** low-frequency harmonic sounds of midshipman toadfish observed at Nine Foot Stake over nighttime periods in April. **C)** low-frequency daytime fish vocalizations common across the western reef sites. **D)** low frequency sounds of recreational boats moored within the Looe Key Preservation Area. **E)** pulsed knocking sounds recorded at the Looe Key during nighttime periods, **F)** spring time dusk choruses of persistent knocking observed at Looe Key, with grouper calls occupying the lower frequency portion of the spectrum. Spectrograms show power spectral density as a function of time and frequency; example A displays frequencies <20 kHz and all other examples (B-F) show

frequencies < 1.5 kHz. Waveform plots are bandpass filtered 5-20 kHz in A and 0.05-1.5 kHz in B-F.

Implications and Future work.

This work establishes a baseline assessment of the soundscape within spur-and-groove coral reef habitats across the Lower Keys Region of the FKNMS. Understanding the patterns of biological sound production as a function of space and time allows us to understand the utilization of these habitats by different marine animals.

The data show that the temporal pattern of high-frequency sound is driven by invertebrate noise, and displays a stable diel pattern that is correlated temporally across the region. The lower frequency soundscape shows greater variability between sites tracking the spatial and temporal distribution of soniferous fish. Future soundscape monitoring efforts may track sound production to identify changes in the prevalence and distribution of different call types to understand fish distribution and abundance patterns, spawning behaviors, and the response of the ecosystems to changing environmental conditions or disturbance events.

Recreational boating appears to be the main source of anthropogenic noise across the Lower Keys Region. The soundscape of the Looe Key Preservation area is dominated by anthropogenic sound during daytime hours throughout most of the summer and fall, as recreational boats make use of the extensive network of mooring buoys in this area. Future work will expand the fusion of acoustic data and remotely sensed imagery to better understand recreational use of reefs within the Florida Keys National Marine Sanctuary, and the merger of passive acoustic data with more traditional ecological approaches, such as reef visual census data. Ongoing efforts to improve and automate call class identification will expand our ability to extract species level information from the passive acoustic records.

(4) Impact of hurricane Irma on the underwater soundscape.

On September 2017, Hurricane Irma (Category 4) traveled across the Lower Florida Keys with sustained hurricane force winds (>64kts) extending 130 km from the center (Cangialosi et al. 2017). Hurricane Irma passed directly over the Florida Keys National Marine Sanctuary (FKNMS) nearshore marine habitats before making landfall near Cudjoe Key, Florida (USA) (Cangialosi et al. 2017, NOAA/RAMMB N. 2017). Short-term impacts by large freshwater inflows resulted in changes in the phytoplankton community in nearby coastal canals, with phytoplankton communities returning to normal seasonal patterns within 3 months after the hurricane (Wachnika et al. 2019). The impacts to the Lower Florida Keys seagrass communities from Irma were generally localized, with species-specific beds of seagrass uprooted, and loss of seagrass from storm water runoff resulting in low dissolved oxygen and persistent hyposalinity, similar to historical datasets (Fourqurean et al. 2004, Wilson et al. 2019). Coral reefs in the Middle and Upper Keys showed a significant decline in abundance of the keystone urchin grazer *Diadema antillarum*, as well as loss of sponges and hydrocorals due to high sedimentation (Kobelt et. al. 2019).

During October 2017, NOAA science divers and partners surveyed more than 50 coral reef sites from Biscayne Bay (near Miami) to the Marquesas (southwest of Key West) and described

severe damage in the Middle and Lower Florida Keys sponge and coral communities from storm force waves, fast-moving debris, and heavy sediment deposits [100]. Sedimentation was the most common impact among sites, resulting in poor visibility and high amounts of marine debris (Viehman et al. 2018). In December 2017, NC State science divers surveyed eight fore-reef sites, including ESB and WDR, and observed poor visibility (<3m), loose rubble, collapsed reef ledges with a mix of schooling species, as well as sedimented and fragmented sub-massive reef-building corals (Fig 15, personal observation K. Simmons). The short-term disturbance in environmental conditions and the remaining fractured reef habitat structure likely impacted marine faunal interactions and behavior; however, little is known about how these changes in the coral reef habitat are reflected in the sound production of coral reef animals that are mobile. Passive acoustic recordings were used to characterize the underwater soundscape of the coral reef tract in the lower Florida Keys, USA before, during and after Hurricane Irma. In the weeks following the storm, the biological sounds produced by fish exhibited similar pre-disturbance temporal patterns, and the high frequency noise associated with snapping shrimp showed only a small shift in its diurnal patterns. This opportunistic study investigates the utility of soundscapes in assessing disturbance impacts to the coral reef soundscape generated by soniferous reef fishes and snapping shrimp within a track of the Florida Keys reef system impacted by Hurricane Irma. The main objectives of this study were to (i) quantify the cumulative acoustic exposure associated with the passage of hurricane Irma, and (ii) identify and quantify temporal changes within the biophony in response to Irma with emphasis on daily and diurnal soundscape patterns.

Methods.

As a part of the overall research program, eight hydrophones were deployed in July 2017 across several marine reserve zones (Figure 1). After the passage of Hurricane Irma (Category 4) in the lower Florida Keys on September 2017, only 2 of 8 hydrophones were recovered: (1) Eastern Sambo, a no-entry reserve, and (2) Western Dry Rocks, which is open to fishing (Fig 2). The other hydrophones were lost, presumably due to wave action and surge from the hurricane. The hydrophone at Western Dry Rocks was recovered after the hurricane lying in sand near the mooring, which removed our ability to use these data to quantitatively assess the post-disturbance soundscape.

Environmental variables. -- Hurricane Irma's track, wind swath and landfall data were accessed from NOAA's National Hurricane Center report on Irma (https://www.nhc.noaa.gov/data/tcr/AL112017_Irma.pdf). Hurricane Irma made landfall near Cudjoe Key in the lower Florida Keys at 08:00 Eastern Standard Time (EST) on September 10, 2017 (Fig 2) before continuing north toward central Florida. Maximum wind speeds reached 115kts with a minimum barometric pressure of 931 hPa at landfall. Barometric pressure data were used, independent of the acoustic time series, to delineate the passage of the storm over the reef. Storm duration was defined as the time window over which the pressure fell and remained below its 2.5% quantile level for data collected between July and October 2017. Barometric pressure data were obtained from the Sand Key Lighthouse, Buoy Station ID SANF1 (24.456°N, 81.877°W), located ~ 5km from WDR. These data were recorded hourly with a standard barometer elevation at 14.6 m above the mean sea level.

Hurricane acoustic energy exposure. - To place the acoustic exposure at these reef sites in context and make comparisons with other sound sources, we quantified the acoustic exposure by

representing all storm related noise as being sourced from a point at the sea surface directly above each hydrophone and calculating the equivalent energy. Over the four-day duration of the storm, the received root mean square SPLs calculated for each file were corrected to acoustic source levels (referenced @ 1m) assuming spherical spreading loss between the sea surface and seafloor. The equivalent acoustic power (J/s) that radiated into the water column (i.e., across a 1 m radius hemisphere with surface area 2π) was then estimated assuming a constant water density (1030 kg/m3) and sound velocity (1485 m/s). The acoustic energy was determined by integrating these power values over the duration of the storm, assuming each two minute file is representative of a surrounding 20 minute time window, and then subtracting the energy that would be calculated if the procedure was repeated using the mean background (pre-storm) noise levels. This energy exposure value can then be compared to the equivalent energy that would be associated with common natural and anthropogenic sources (e.g. fishing vessels) operating over a set duration if these sources were fixed in position at the sea surface directly above the hydrophone. This value, however, does not represent the total acoustic energy imparted by the storm.

Acoustic data collection and analyses. - Fish sounds occupy the low-frequency spectrum (<50Hz to several kHz), often competing with background environmental noise (i.e. wind, wave action) in similar frequency bands]. Sound Pressure Levels (SPLs) were calculated at several frequency bands of ecological interest: (1) a low frequency band L1 (50-300Hz) representative of the fish families Serranidae, Holocentridae, and Pomacentridae, (2) a low frequency band L2 (1.2-1.8kHz) representative of Haemulidae, Lutjanidae, Scaridae, Sciaenidae, and (3) a high frequency band H (7-20kHz) representative of snapping shrimp (Alpheidae), which are a dominant sound producer in coral reef habitats.

Results.

Environmental variables. - Barometric pressure data exhibited semidiurnal oscillations characteristic of the Florida Keys region (Fig 16A). The passage of the storm is marked by a period of low (< 1011 hPa) barometric pressure, which extends from ~12:00 on September 8, 2017 to ~12:00 September 12, 2017 (4 days), reaching a trough at 966 hPa on September 10, 2017 at 06:50 (all times EST). In analyzing the soundscape during the pre- and post-storm windows, a 1-day buffer was applied on either side of the hurricane, such that the pre-storm period ends on September 7th at 12:00 and the post-storm period begins on September 13th at 12:00.

Before and after the storm, daily bottom temperatures at WDR and ESB varied between 26-28°C, except for a short period of slightly increased temperatures at ESB between August 15 to August 19, 2017, which was likely influenced by the lunar spring tide. Both sites exhibited a sharp decline in bottom temperature reaching 25°C shortly after the hurricane made landfall. (Fig 16B). Post-hurricane, cooler water temperatures remained a few days longer at ESB than WDR before returning to pre-disturbance daily temperature oscillations.

Hurricane acoustic energy exposure. - Hurricanes represent broadly distributed acoustic sources, with the sounds recorded at each hydrophone arriving from a range of azimuths and incidence angles. However, to place the acoustic exposure at these reef sites in context and make

comparisons with other sound sources, we quantified the acoustic exposure by representing all storm related noise as being sourced from a point at the sea surface directly above each hydrophone and calculating the equivalent energy. WDR experienced a higher cumulative energy exposure than ESB estimated at 9.9 x 103 J and 4.8 x 103 J, respectively. In comparison to other acoustic energy disturbances commonly experienced in the lower Florida Keys region, the exposure over the duration of Hurricane Irma was comparable to small vessel (SL = 153 dB re 1μPa @ 1m) operating continuously directly overhead for 1 week (ESB) to 2 weeks (WDR). The WDR hydrophone presumably detached from its mooring at some point during the storm; however, the exact timing of this event was not readily identifiable, and no corrections were made to account for potential changes in sensitivity of the instrument. Estimates of acoustic exposure also do not account for the signals produced by debris impacting the hydrophone and mooring, since this effect is not easily disentangled from the acoustic wavefield.

Acoustic data collection and analyses. - Both sites showed temporal patterns in the biophony evident with their long-term spectrograms (see Fig. 18 for ESB). A daily pattern of fish vocalizations within the L1 frequency band was apparent at WDR and ESB over the ~2 month recording period before the hurricane, with increased sound levels around the full moons in August and September (See Fig. 18 for ESB). Fish calls within both low frequency bands were masked or absent during the storm, before reappearing immediately after the storm (See Fig. 18 for ESB). The L2 band captured broadband fish calls, including the upper range of pulsated "grunts" (>1000Hz) and aggregated "knocks" between 1200-2500Hz, as well as including the lower range of snapping shrimp sound production in the high frequency band. Snapping shrimp activity within the H band persisted before and after the storm at both sites (Simmons et al. 2020).

The daily patterns in SPLs before and after the storm were examined for the ESB site. Within the three frequency bands, trimmed means were calculated for each recording interval (00:00, 00:20… 23:40) over the 18- and 24-day windows capturing the same portion of the lunar cycle before and after the storm. The results for the 18-day windows are displayed in Fig 19, along with their bootstrapped confidence intervals. The dominant temporal pattern was a diurnal rhythm (day vs. night) in sound production, along with a small increase in high frequency noise during crepuscular periods. The daily pattern of low and high frequency sound production was largely maintained after the storm, with only small shifts in the average loudness. Within the L1 band, a small decrease in the average SPL is observed during the nighttime hours, with little change in the average level during the daytime hours. For the L2 band, a small decrease in the average SPL is observed during the daytime hours, with little change observed at night.

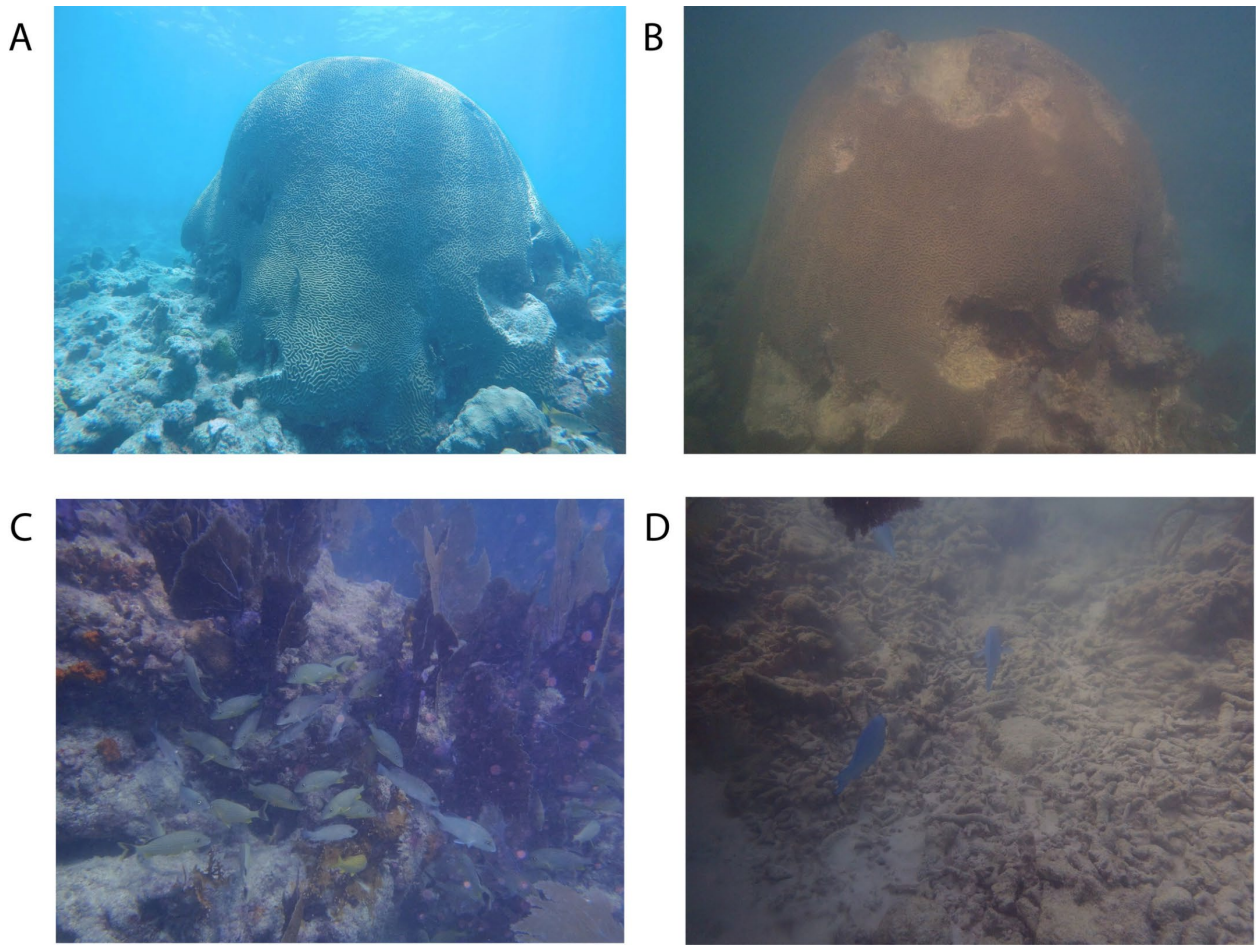

Figure 15. Before-After impacts of hurricane Irma on coral reefs in the Florida Keys, with Before images taken in August 2017 and After images taken in December 2017. (A) Brain coral at Eastern Sambo study site taken in August 2017 and (B) its structural damage after Irma in December 2017. (C) Divers observed fish aggregations near and underneath collapsed reef ledges at Looe Key reef (~26 km northeast of Eastern Sambo study site), and the (D) same site with high amounts of reef rubble after Irma. Photo credit K. Simmons.

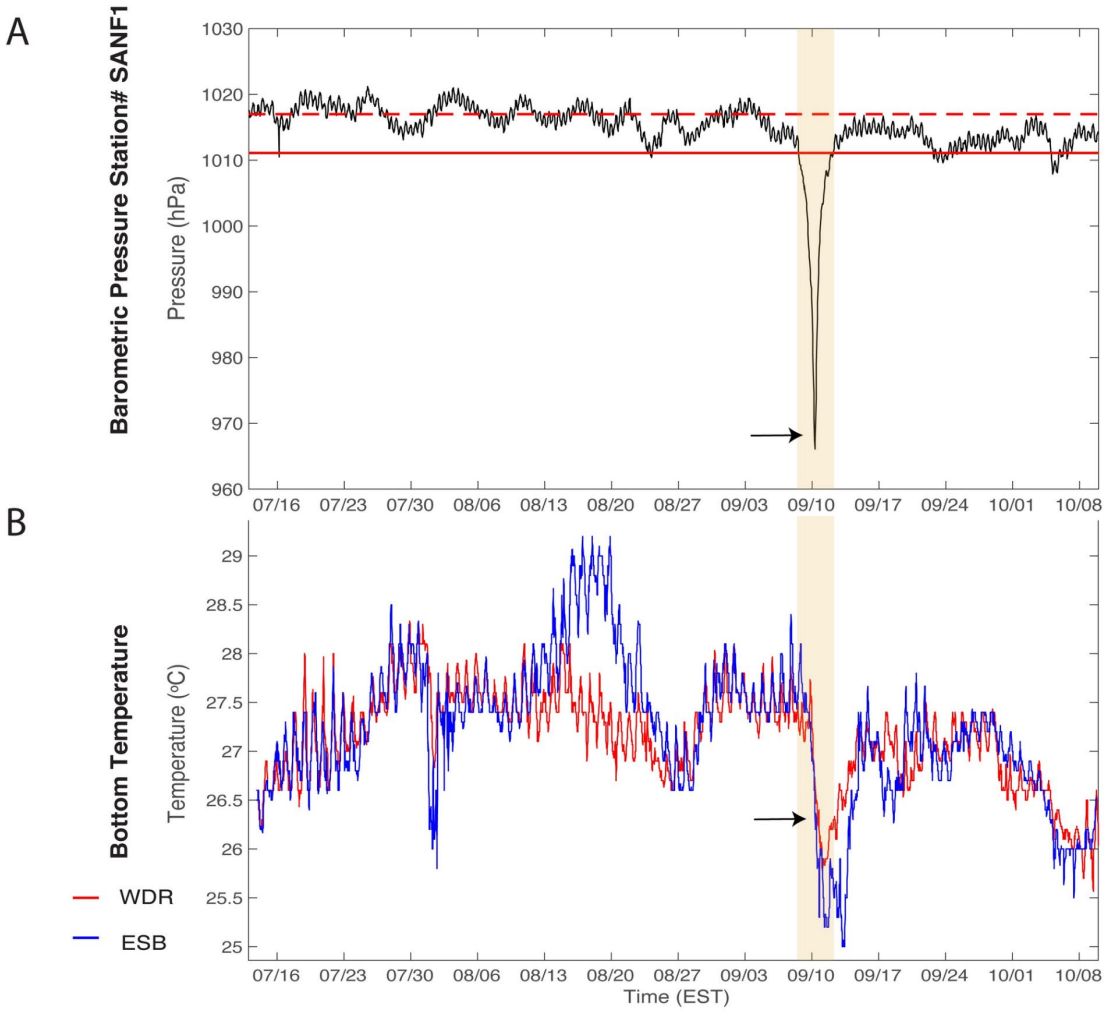

Fig 16. Environmental Data. (A) Barometric pressure data from Sand Key Lighthouse, FL (Station ID SANF1 24.456°N, 81.877°W) NOAA-National Data Buoy Center is shown as a black line with the median (dashed red) and the lower 2.5% confidence interval (solid red). (B) Mean hourly bottom temperature (°C) from hydrophone sensor for Western Dry Rocks (red) and Eastern Sambo (blue). The orange bar represents Hurricane Irma duration and the black arrow indicates the times of landfall at Cudjoe Key FL on September 10, 2017 08:00 EST.

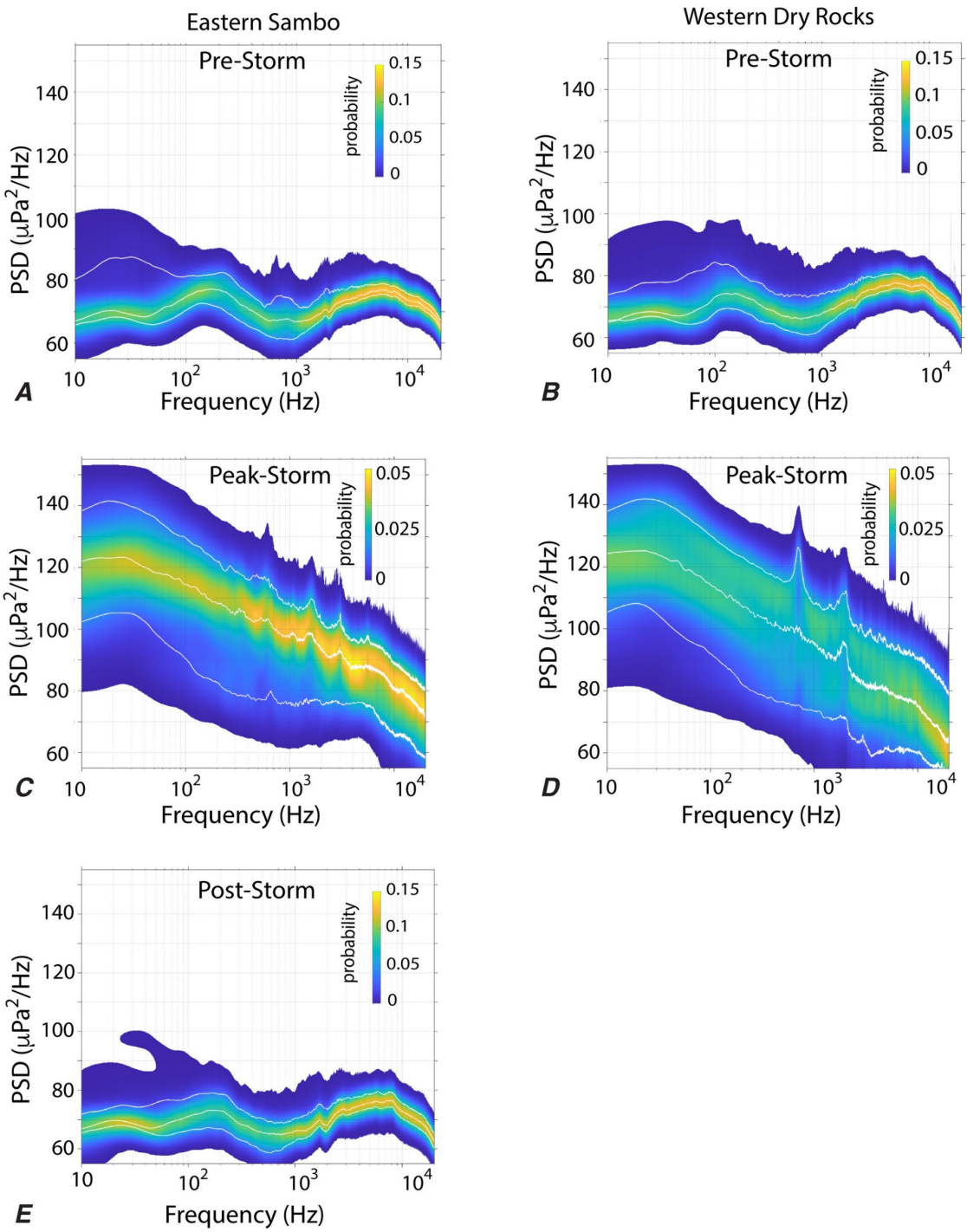

Fig 17. Power spectral density (PSD) plot. Power spectral density plot of Eastern Sambo (left) and Western Dry Rocks (right) pre-storm (A, B), peak-storm (C, D), and post-storm (E). The colors show the probability distribution of the spectral amplitudes, and white lines show the 5, 50, and 95% quantiles of power spectral density as a function of frequency.

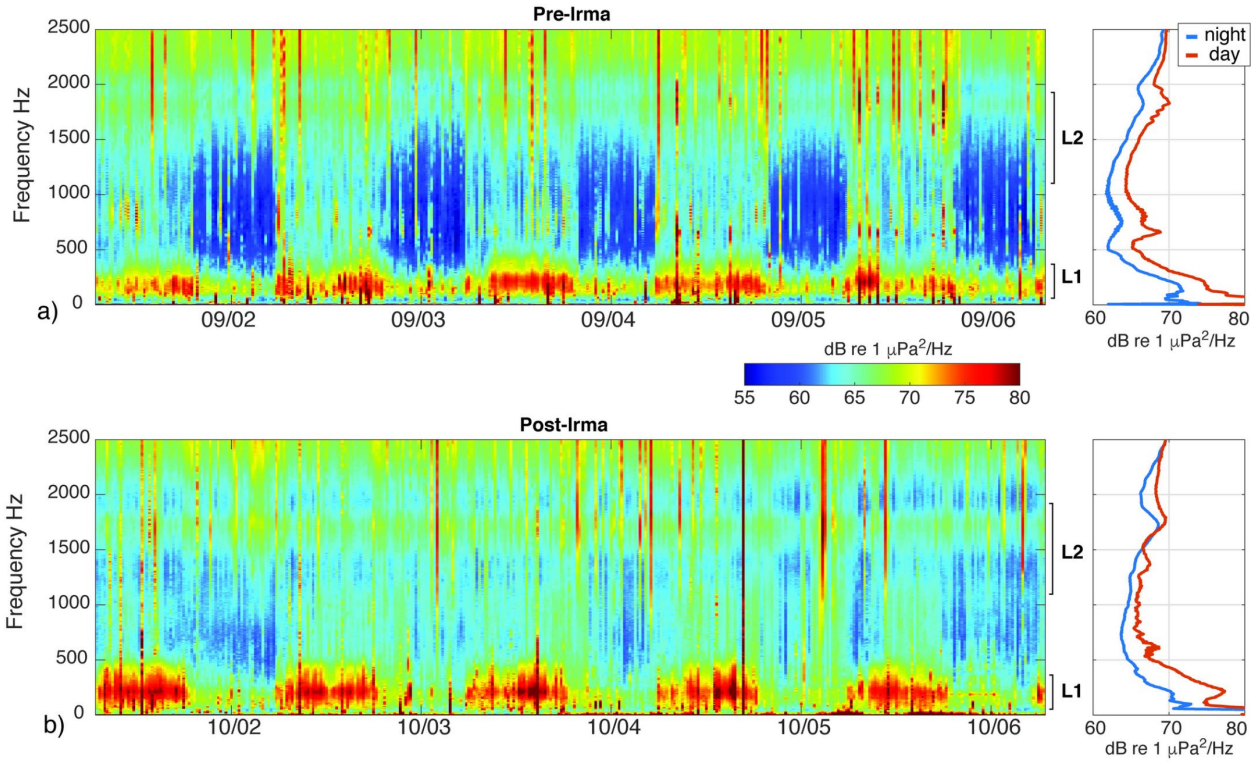

Fig 18. Short-duration spectrograms from Eastern Sambo. Spectrograms displaying the low frequency patterns of sound production during 5-day windows around the full moons that occurred (a) before and (b) after the passage of Hurricane Irma. Spectrograms are derived using the average spectra with each two minute recording. Time-axis ticks indicate midnight EST. Sound pressure levels are elevated during daytime hours, relative to the nighttime hours. The daily pattern of sound production reflects the acoustic activity and/or presence of multiple species (see call example in Fig S1). The diurnal pattern in low-frequency (L1) sound production is present before and after the storm. The diurnal pattern of mid-frequency (L2) sound production is a less pronounced, and appears to weaken after the passage of the storm. Panels on the right show average sound pressure levels during daytime and nighttime recordings averaged over the 5-day windows.

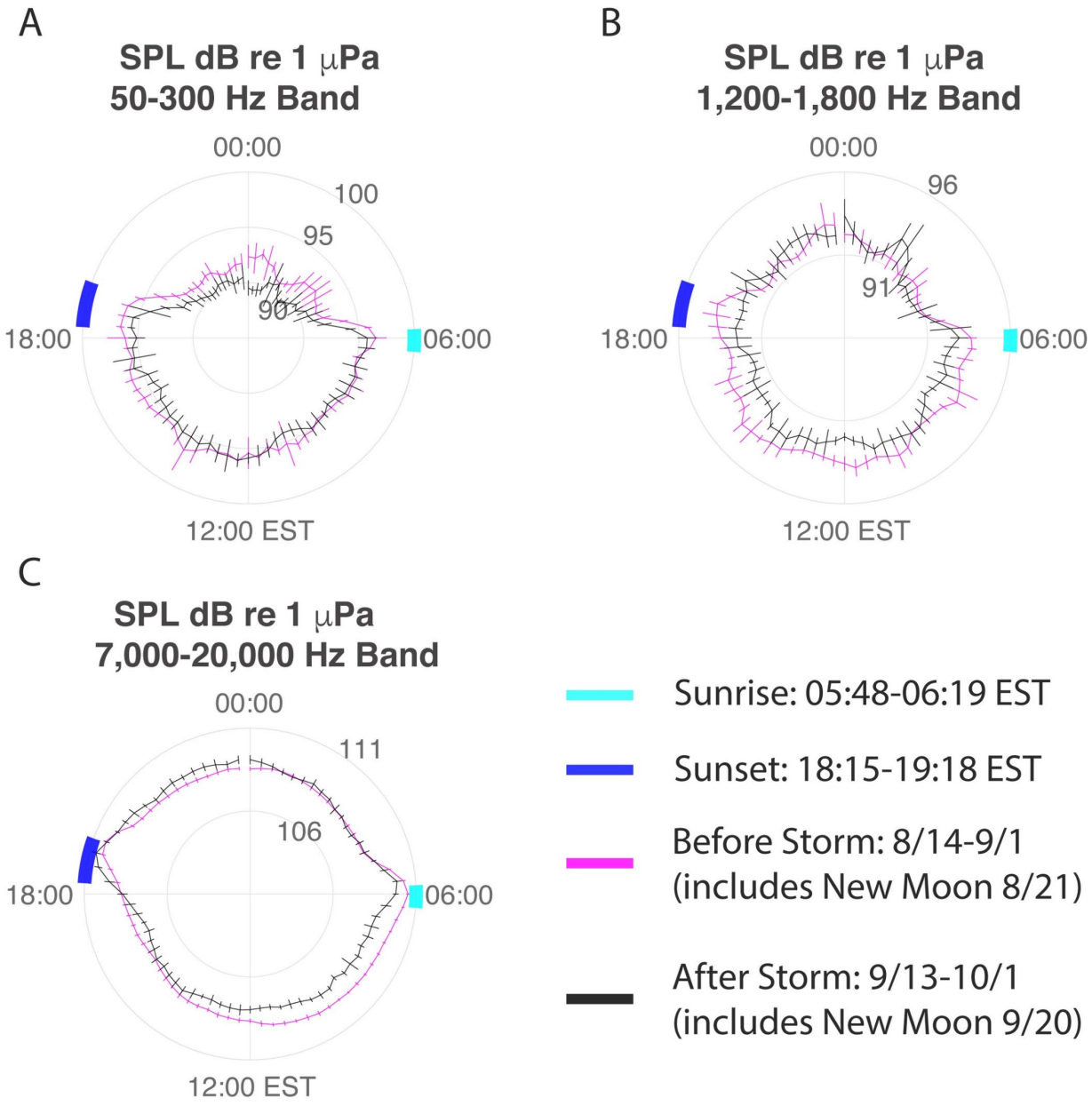

Fig 19. Polar diagram for Eastern Sambo. Polar diagram of Sound Pressure Levels (SPLs) for ESB for the 18-day observation window before (magenta) and after (black) the hurricane. Means for each recording interval are shown with 3-point moving average. Error bars represent the 68% confidence interval of mean. Data are displayed for A) L1 frequency band (50-300Hz); B) L2

frequency band (1,200-1,800Hz); and C) H frequency band (7,000-20,000Hz). Local sunrise (05:48-06:19 EST) and sunset (18:15-19:18 EST) times during the deployment are shown in cyan and blue, respectively.

Implications.

This study suggests that on short time scales, temporal patterns in the coral reef soundscape were relatively resilient to acoustic energy exposure during the storm, as well as changes in the benthic habitat and environmental conditions resulting from hurricane damage.

g. Literature Cited

Allison, G.A., Lubchenco, J., & Carr, M.H. 1998. Marine reserves are necessary but not sufficient for marine conservation. *Ecological Applications,* 8:S79-S92.

Alvarez-Filip, L., Dulvy, N.K., Cotê, I.M., Watkinson, A.R., Gill, J.A. 2011. Coral identity underpins architectural complexity on Caribbean reefs. *Ecological Applications* 21:2223–2231.

Alvarez-Filip L, Carricart-Ganivet JP, Horta-Puga G, Iglesias-Prieto R. 2013. Shifts in coral-assemblage composition do not ensure persistence of reef functionality. *Science Reports* 3:3486.

Aronson, R. B., W. F. Precht. 1995. Landscape patterns of reef coral diversity: a test of the intermediate disturbance hypothesis. *Journal of Experimental Marine Biology and Ecology*, *192*(1):1-14.

Ault, J.S., Smith, S.G., Bohnsack, J.A., Luo, J., Harper, D.E., & McClellan, D.B. 2006. Building sustainable fisheries in Florida's coral reef ecosystem: positive signs in the Dry Tortugas. *Bulletin of Marine Science,* 78:633–654.

Bartholomew, A., J. A. Bohnsack, S. G. Smith, J. S. Ault, D. E. Harper and D. B. McClellan. 2008. Influence of marine reserve size and boundary length on the initial response of exploited reef fishes in the Florida Keys National Marine Sanctuary, USA. *Landscape Ecology* 23:55-6

Bass, A. H. (1990). Sounds from the intertidal zone: Vocalizing fish. *BioScience*, *40*(4), 249–258. https://doi.org/10.2307/1311261

Bohnsack, J.A. & Ault, J.S. 1996. Management strategies to conserve marine biodiversity. *Oceanography,* 9:73-82.

Bozec, Y., Alvarez-Filip L., Mumby, P.J. 2015. The dynamics of architectural complexity on coral reefs under climate change. *Global Change Biology* 21:223-235. Doi:10.1111/gcb.12698.

Brandt, M.E., Zurcher, N., Acosta, A., Ault, J.S., Bohnsack, J.A., Feeley, M.W., Harper, D.E., Hunt, J., Kellison, G.T., McClellan, D.B., Patterson, M.E., & Smith, S.G. 2009. A cooperative multi-agency reef fish monitoring protocol for the Florida Keys coral reef ecosystem. *Natural Resource Report NPS/SFCN/NRR—2009/150*. National Park Service, Fort Collins, Colorado.

Burns, J., A. Fukunaga, K. Pascoe, A. Runyan, B. Craig, J. Talbot, A. Pugh, R. Kosaki. 2019. 3D habitat complexity of coral reefs in the northwestern Hawaiian Islands is driven by habitat complexity of coral reefs in the Northwestern Hawaiian Islands is driven by coral assemblages structure. International Archives of the Photogrammetry, Remote Sensing

and Spatial Information Sciences. XLII-2/W10. 61-67. 10.5194/isprs-archives-XLII-2-W10-61-2019.

Cangialosi J. P., Latto A. S., Berg R. 2017. Tropical Cyclone Report: Hurricane Irma. 2017. (AL112017): 30 August – 12 September 2017. National Center Tropical Cyclone Report. 2018;111.

Darling E. S., Alvarez-Filip L, Oliver T. A., McClanahan T. R., Côte I. M. 2012. Evaluating life-history strategies of reef coral from species traits. *Ecology Letters* 15:1378-1386.

Darling E. S., Graham N. A. J., Januchowski-Hartley F. A., Nash K. L., Pratchett M. S., Wilson S. K. 2017. Relationships between structural complexity, coral traits, and reef fish assemblages. *Coral Reefs* 36:561-575 . doi:10.1007/s00338-017-1539-z.

Ferrari, R., McKinnon, D., He, H., Smith, R. N., Corke, P., González-Rivero, M., Mumby, P. J. and Upcroft, B. 2016. Quantifying multiscale habitat structural complexity: a cost effective framework for underwater 3D modelling. *Remote Sensing*, 8(2), p.113

Fourqurean J. W., Rutten L. M. 2004. The impact of Hurricane Georges on soft-bottom, back reef communities: site- and species-specific effects in south Florida seagrass beds. Bulletin of Marine Science. 75(2):239-257.

Fukunaga, A., J. Burns, B. Craig, R. Kosali. 2019. Integrating three-dimensional benthic habitat characterization techniques into ecological monitoring of coral reefs. J. Mar. Sci. Eng. 7, 27; doi:10.3390/jmse7020027

Gardmark, A., Jonzén, N., & Mangel, M. 2006. Density-dependent body growth reduces the potential of marine reserves to enhance yields. *Journal of Applied Ecology*, 43:61-69.

Goergen, E.A., S. Schopmeyer, A.L. Moulding, A. Moura, P. Kramer, and T.S. Viehman. 2020. Coral reef restoration monitoring guide: Methods to evaluate restoration success from local to ecosystem scales. NOAA Technical Memorandum NOS NCCOS 279. Silver Spring, MD. 145 pp. doi: 10.25923/xndz-h538

Halpern, B.S. 2003. The impact of marine reserves: do reserves work and does reserve size matter? *Ecological Applications,* 13:S117-S137.

Keller, B.D., S. Donahue (eds). 2006. 2002-03 sanctuary science report: an ecosystem report card after five years of marine zoning. U.S. Department of Commerce, National Oceanic and Atmospheric Administration, National Ocean Service, Office of National Marine Sanctuaries, Florida Keys National Marine Sanctuary, Marathon, FL.

Kobelt J. N., Sharp W. C., Miles T. N., Feehan C. J. 2019. Localized impacts of Hurricane Irma on *Diadema antillarum* and coral reef community structure. Estuaries and Coasts. Nov 15:1-1. Doi:10.1007/s12237-019-00665-4.

Kramer, K. L., K. L. Heck. 2007. Top-down trophic shifts in Florida Keys patch reef marine protected areas. *Marine Ecology Progress Series* 349:111-123.

Lindseth A. V., P. S. Lobel. 2018. Underwater soundscape monitoring and fish bioacoustics: A review. *Fishes*, 3.36: doi:10.3390/fishes3030036

Locascio, J.V., Burton, M.L 2016. A passive acoustic survey of fish sound production at Riley's Hump within Tortugas South Ecological Reserve: implications regarding spawning and habitat use. *Fishery Bulletin,* 114:103-116.

Locascio, J.V. & D. Mann. 2008. Diel periodicity of Fish Sound Production in Charlotte Harbor, Florida. *Transactions of the American Fisheries Society* 137:606-615.

Lubchenco, J., Palumbi, S.R., Gaines, S.D. & Andelman, S. 2003. Plugging a hole in the ocean: the emerging science of marine reserves. *Ecological Applications,* 13:S3-S7.

Ludford, A., V. J. Cole, F. Porri, C. D. McQuaid, M. D. Nakin, and J. Erlandsson 2012. Testing

source-sink theory: the spill-over of mussel recruits beyond marine protected areas. *Landscape Ecology* 27(6), 859-868.

Lugli, M., Pavan, G. & Torricelli, P. 1986. The importance of breeding vocalizations for mate attraction in a freshwater goby with composite sound repertoire. *Ethology Ecology & Evolution Journal,* 8: 343–351.

Mann, D.A., Locascio, J.V., Coleman, F.C. & Koenig, C.C. 2009. Goliath grouper *Epinephelus itajara* sound production and movement patterns on aggregation sites. *Endangered Species Research,* 7: 229−236.

Mann, D. A., Locascio, J. V., Schärer, M. T., Nemeth, M. I., R. S. Appledoorn. 2010. Sound production by red hind *Epinephelus guttatus* in spatially segregated spawning aggregations. *Aquatic Biology,* 10:149-154.

Maynard, J., J. Byrne, K. Kerrigan, D. Tracey, K. Bohnsack, F. Pagan, J. Walczak, G. Williams. 2017. Coral reef resilience to climate change in the Florida Reef Tract. Florida Department of Environmental Protection. Miami, FL, pp.1-30.

McClanahan, T. R., N. Graham, M. MacNeil, N. Muthiga, J. Cinner, J. Bruggemann, S. Wilson. (2012). Critical thersholds and tangible targets for ecosystem-based management of coral reef fisheries. *Proceedings of the National Academy of Sciences USA,* 108:17230-17233.

Montie, E. W., S. Vega and M. Powell. 2015. Seasonal and spatial patterns of fish sound production in the May River, South Carolina. *Transactions of the American Fisheries Society*. 144:705–716. doi: 10.1080/00028487.2015.1037014.

Myrberg, Jr., A. A., M. Mohler and J. Catala. 1986. Sound production by males of a coral reef fish (*Pomacentrus partitus*): its significance to females. *Animal Behavior,* 24: 923–933.

Natural Resource Council. 2015. Sea Change: 2015-2025. Decadal Survey of Ocean Sciences, Washington, DC, The Academies Press, pp 134.

Nelson, M.D., Koenigh, C.C., Coleman, F.C., & Mann, D.A. 2011. Sound production of red grouper *Epinephelus morio* on the West Florida Shelf. *Aquatic Biology,* 12:97-108.

Nemeth, R. S., Blondeau J., Herzlieb S., and Kadison E. 2007. Spatial and temporal patterns of movement and migration at spawning aggregations of red hind, *Epinephelus guttatus*, in the U.S. Virgin Islands. *Environmental Biology of Fishes,* 78:365−381.

NOAA/RAMMB N. 2017. Aircraft-based tropical cyclone surface wind analysis. In AL112017-major hurricane Irma: Regional and mesoscale meteorology branch. National Oceanic and Atmospheric Administration. 2017.

Nunes, V., G. Pawlak. 2008. Observations of bed roughness of a coral reef. *Coastal Research* 24(10024):39-50. Doi:10.2112/05-0616.1

Peters, J., D. Eggleston, B. Puckett and S. Theuerkauf. 2017. Oyster demographics in harvested reefs versus no-take reserves: Implications for larval spillover and restoration success. *Frontiers in Marine Science, Conservation & Sustainability* .4:326. Doi:10.3389/fmars.2017.00326.

Phinn S. R., Roelfsema C. M., Mumby P. J. 2012. Multi-scale, object-based image analysis for mapping geomorphic and ecological zones on coral reefs. *International Journal of Remote Sensing*, 33:12, 3768-3797, DOI: 10.1080/01431161.2011.633122

Pittman, S. K.L. Yates, P.J. Bouchet, D. Alvarez-Berastegui, S. Andréfouët, S.S. Bell, C. Berkström, C. Boström, C.J. Brown, R.M. Connolly, R. Devillers, D. Eggleston, & 26 other co-authors. 2021. Seascape ecology: Identifying research priorities for an emerging ocean sustainability science. *Marine Ecology Progress Series*. 663:1-20.

Royer, J. P., Nawaf, M. M., Merad D., Saccone M., Bianchimani, O., Garrabo, J. Ledoux J-B., Lopez-Sanz A., Drap P. 2018. Photogrammetric surveys and geometric processes to analyses and monitor red coral colonies. *Journal of Marine Science and Engineering*, 6:52. Doi:10.3390/jmse6020042.

Rowell, T.J., Schärer, M.T., Appledoorn, R.S., Nemeth, M.I., Mann, D.A., & Rivera, J.A. 2012. Sound production as an indicator of red hind density at a spawning aggregation. *Marine Ecology Progress Series,* 462:241-250

Ruzicka, R.R., Colella, M.A., Porter, J.W., Morrison, J.M., Kidney, J.A., Brinkhuis, V., Lunz, K.S., Macaulay, K.A., Bartlett, L.A., Meyers, M.K., J. Colee. 2013. Temporal changes in benthic assemblages on Florida Keys reefs 11 years after the 1997/1998 El Niño. *Marine Ecology Progress Series*, *489*, pp.125-141.

Sale, P. F., Cowen, R. K., Danilowics, B. S., Jones, G. P., Kritzer, J. P., Lindeman, K. C., Planes, S., Polunin, N.V.C., Russ, G. R., Sadovy, Y. J., Steneck, R.S. 2005 Critical science gaps impede use of no-take fishery reserves. *Trends in Ecology & Evolution*, 20:74–80.

Schärer, M. T., Nemeth, M. I., Mann, D., Locascio, J., Appeldoorn, R. S., Rowell T. J. 2012. Sound production and reproductive behavior of Yellowfin grouper *Mycteroperca venenosa* (Serranidae) at a spawning aggregation. *Copeia,* 2012:136-145.

Schärer, M. T., Nemeth, M. I., Rowell, T. J., & Appledoorn, R. S. 2013. Sounds associated with the reproductive behavior of the black grouper *(Mycteroperca bonaci*). *Marine Biology,* 161:141-147.

Shaver E C, Courtney C A, West J M, Maynard J, Hein M, Wagner C, Philibotte J, MacGowan P, McLeod I, Boström-Einarsson L, Bucchianeri K, Johnston L, Koss J. 2020. A Manager's Guide to Coral Reef Restoration Planning and Design. NOAA Coral Reef Conservation Program. NOAA Technical Memorandum CRCP 36, 128 pp.

Simmons, K., D. Eggleston and D. Bohnenstiehl. (2021). Hurricane impacts on a coral reef soundscape. *PLoS ONE* 16(2): e0244599. https://doi.org/10.1371/journal.

Slabbekoorn H., Bouton N., van Opzeeland I., Coers A., Cate C., Popper A. N. 2010. A noisy spring: the impact of globally rising underwater sound levels on fish. Trends Ecol. Evol. 25, 419– 427. (doi:10. 1016/j.tree.2010.04.005).

Tidau S., Briffa M. 2016. Review on behavioral impacts of aquatic noise on crustaceans. Proceedings of Meetings on Acoustics. 27. 010028. 10.1121/2.0000302.

Tupper, M., M. Rudd. 2002. Species-specific impacts of a small marine reserve on reef fish production and fishing productivity in the Turks & Caicos Islands. *Environmental Conservation,* 29:2484-492.

Valles, H., Sponaugle, S., & Oxenford, H.A. 2001. Larval supply to a marine reserve and adjacent fished area in the Soufriere Marine Management Area, St. Lucia, West Indies.

Versluis M., Schmitz B., von der Heydt A., Lohse D. 2000. How snapping shrimp snap: through cavitating bubbles. Science 289: 2114−2117.

Viehman, S., S. Gittings, S. Groves, J. Moore, T. Moore, J. Stein. 2018. NCCOS Assessment: Coral Disturbance Response Monitoring (DRM) along the Florida Reef Tract following Hurricane Irma from 2017-10-09 to 2017-10-18 (NCEI Accession 0179071). NOAA National Centers for Environmental Information. Dataset. doi:10.25921/sscd-6h41.

Wachnicka A., Browder J., Jackson T., Louda W., Kelbe C., Abdelrahman O., et al. 2019. Hurricane Irma's impact on water quality and phytoplankton communities in Biscayne Bay (Florida, USA). Estuaries and Coasts. Doi: 10.1007/s12237-019-00592-4.

Wilson S. S., Furman B. T., Hall M. O., Fourqurean J. W. 2019. Assessment of Hurricane Irma impacts on south Florida seagrass communities using long-term monitoring programs. Estuaries and Coasts. 2019; Jan:1-4. Doi:10.1007/s12237-019-00623-0.

Young, G. C., Dey, S., Rogers, A. D., Exton, D. 2017. Cost and time-effective method for multi-scale measures of rugosity, fractal dimension, and vector dispersion from coral reef 3D models. PLoS ONE 13(7):e0201847.

Zawada, K. J. A., Madin, J. S., Baird, A. H., Bridge, T. C. L, Dornelas, M. 2019. Morphological traits can track coral reef responses to the Anthropocene. *Functional Ecology* 33: 962– 975. https://doi-org.prox.lib.ncsu.edu/10.1111/1365-2435.13358

Appendices.

Table 1. Mean fish density from RVC diver surveys according to Family and Sampling Date for Eastern Sambo (Special Use, Research Only Area, SUA).

Eastern Sambo (SUA)	Feb-17	May-17	July-17	Dec-17	Jun-18	Sep-18	Dec-18
Acanthuridae	0.667	2.000	4.000	15.500	2.000	1.000	1.000
Apogonidae	0.333	-	-	-	-	-	-
Aulostomidae	0.333	-	-	-	-	-	-
Carangidae	4.333	0.500	-	-	3.000	1.000	-
Centropomidae	-	-	-	-	-	-	-
Chaetodontidae	1.000	1.000	2.500	-	-	4.000	1.500
Dasyatidae	-	-	-	-	-	-	-
Echeneidae	-	-	-	-	-	-	-
Ephippidae	-	-	-	-	-	-	-
Gerreidae	-	-	-	-	-	-	-
Ginglymostomatidae	-	-	-	-	-	-	-
Gobiidae	-	0.500	-	-	-	-	-
Grammatidae	-	-	-	-	-	-	-
Haemulidae	13.000	7.000	8.000	30.500	1.000	10.500	43.500
Holocentridae	0.667	2.000	1.000	1.500	-	1.000	3.000
Kyphosidae	3.333	-	3.000	0.500	-	-	1.000
Labridae	55.667	49.500	29.500	11.500	35.500	24.000	50.500
Lutjanidae	23.333	10.500	7.500	21.000	16.500	19.000	5.500
Monacanthidae	-	-	-	-	-	-	0.500
Mullidae	-	1.000	-	-	-	-	-
Muraenidae	-	-	-	-	-	-	-
Ostraciidae	-	-	0.500	-	-	-	-
Palinuridae	-	-	-	-	-	-	-
Pomacanthidae	34.667	50.500	54.500	14.000	6.500	13.000	38.000
Priacanthidae	-	-	-	-	-	-	-
Scaridae	6.333	12.500	12.500	7.500	13.000	4.000	5.500
Sciaenidae	-	-	-	-	-	-	-
Scombridae	-	-	-	-	-	-	-
Scorpaenidae	-	-	-	-	-	-	-
Serranidae	0.667	-	1.000	1.500	0.500	-	1.000
Sparidae	-	-	-	-	-	-	-
Sphyraenidae	-	-	0.500	0.500	-	-	-
Tetraodontidae	-	-	-	-	-	-	-

Table 2. Mean fish density from RVC diver surveys according to Family and Sampling Date for Looe Key (Special Use, Research Only Area, SUA).

Looe Key (SUA)	Feb-17	May-17	July-17	Dec-17	Jun-18	Sep-18	Dec-18
Acanthuridae	3.000	1.000	2.000	1.750	3.500	2.500	0.500
Apogonidae	-	-	-	-	-	-	-
Aulostomidae	-	-	-	0.250	-	-	-
Carangidae	25.000	1.000	-	-	-	27.000	-
Centropomidae	-	-	-	-	-	-	-
Chaetodontidae	1.500	8.000	1.000	0.750	3.500	4.500	2.000
Dasyatidae	-	-	-	-	-	-	0.500
Echeneidae	-	-	-	-	-	-	-
Ephippidae	-	-	-	-	-	-	-
Gerreidae	-	4.000	-	-	-	-	-
Ginglymostomatidae	-	-	-	-	-	-	-
Gobiidae	-	-	-	-	-	-	-
Grammatidae	-	-	-	-	-	-	-
Haemulidae	6.000	5.000	2.000	144.750	32.000	21.000	15.000
Holocentridae	-	-	-	-	-	-	-
Kyphosidae	-	-	-	0.250	-	-	-
Labridae	23.500	29.500	13.000	21.000	10.000	19.000	2.500
Lutjanidae	17.500	2.500	7.000	23.000	8.000	55.500	8.000
Monacanthidae	-	-	-	-	-	-	-
Mullidae	-	-	-	0.750	-	-	-
Muraenidae	-	-	-	-	-	-	-
Ostraciidae	-	-	-	-	-	-	-
Palinuridae	-	-	-	-	-	-	-
Pomacanthidae	10.000	10.500	6.500	5.000	5.500	9.000	6.500
Priacanthidae	-	-	-	-	-	-	-
Scaridae	12.000	6.000	19.000	4.750	1.000	6.000	-
Sciaenidae	-	-	1.000	0.250	-	-	0.500
Scombridae	2.000	-	-	-	1.000	-	-
Scorpaenidae	-	-	-	-	-	-	-
Serranidae	2.500	1.500	1.000	0.750	0.500	-	-
Sparidae	-	1.000	-	-	-	-	-
Sphyraenidae	-	-	0.500	-	-	-	-
Tetraodontidae	-	0.500	-	-	0.500	-	-

Table 3. Mean fish density from RVC diver surveys according to Family and Sampling Date for Looe Key (Sanctuary Preservation Area, SPA).

Looe Key (SPA)	Feb-17	May-17	July-17	Dec-17	Jun-18	Sep-18	Dec-18
Acanthuridae	5.000	11.500	2.000	4.000	1.000	2.000	0.500
Apogonidae	-	-	-	-	-	-	-
Aulostomidae	0.500	-	-	-	-	-	-
Carangidae	3.500	-	5.500	0.500	-	-	8.500
Centropomidae	-	-	-	-	-	-	0.500
Chaetodontidae	0.500	2.000	1.500	2.750	3.000	2.500	2.000
Dasyatidae	-	0.500	-	-	-	-	-
Echeneidae	-	-	-	-	-	0.500	-
Ephippidae	-	0.500	4.000	-	-	-	-
Gerreidae	-	-	-	-	-	-	-
Ginglymostomatidae	-	-	-	-	-	-	-
Gobiidae	-	-	-	-	0.500	-	-
Grammatidae	-	0.500	-	-	-	-	-
Haemulidae	1.000	1.000	1.500	6.250	1.500	5.500	3.500
Holocentridae	-	0.500	-	-	-	-	-
Kyphosidae	0.500	-	3.000	-	-	-	-
Labridae	23.500	46.500	44.500	29.500	33.000	12.000	13.500
Lutjanidae	20.000	5.000	37.000	29.750	47.500	55.500	85.000
Monacanthidae	0.500	0.500	-	-	-	-	-
Mullidae	-	-	-	-	0.500	0.500	-
Muraenidae	-	-	-	-	-	-	-
Ostraciidae	-	-	0.500	-	-	-	0.500
Palinuridae	-	-	-	-	-	-	-
Pomacanthidae	58.000	33.000	62.500	10.500	4.000	34.500	29.500
Priacanthidae	-	-	-	-	-	-	-
Scaridae	9.000	6.500	4.000	6.000	3.000	10.500	1.500
Sciaenidae	-	-	-	-	-	-	-
Scombridae	2.000	-	-	0.250	-	-	-
Scorpaenidae	0.500	-	-	0.500	-	-	-
Serranidae	1.000	0.500	0.500	0.500	0.500	1.000	-
Sparidae	-	-	0.500	-	-	0.500	-
Sphyraenidae	-	1.000	-	-	-	-	-
Tetraodontidae	-	1.000	-	-	0.500	-	-

Table 4. Mean fish density from RVC diver surveys according to Family and Sampling Date for Sand Key (Sanctuary Preservation Area, SPA).

Sand Key (SPA)		May-17	July-17	Dec-17	Jun-18	Sep-18	Dec-18
	Acanthuridae	4.667	8.000	7.500	40.000	3.000	2.000
	Apogonidae	-	-	-	-	-	-
	Aulostomidae	-	-	0.500	-	-	-
	Carangidae	18.333	-	-	0.500	24.000	-
	Centropomidae	-	-	-	-	-	-
	Chaetodontidae	2.000	1.000	1.000	1.000	1.000	-
	Dasyatidae	-	-	-	-	-	-
	Echeneidae	-	-	-	-	-	-
	Ephippidae	-	-	-	-	-	-
	Gerreidae	-	-	-	-	-	-
	Ginglymostomatida	-	-	-	-	-	-
e	Gobiidae	-	-	-	0.500	-	-
	Grammatidae	-	-	-	-	-	-
	Haemulidae	14.000	14.500	28.000	1.000	5.000	68.500
	Holocentridae	0.333	1.500	1.500	-	-	1.500
	Kyphosidae	-	3.000	3.000	0.500	0.500	5.000
	Labridae	86.000	96.000	23.000	8.500	1.000	5.000
	Lutjanidae	18.667	17.500	30.500	6.000	108.500	14.500
	Monacanthidae	-	-	-	-	-	-
	Mullidae	-	-	1.000	-	0.500	-
	Muraenidae	-	-	-	-	-	-
	Ostraciidae	-	-	-	-	-	-
	Palinuridae	-	0.500	-	-	-	-
	Pomacanthidae	13.000	14.000	23.500	8.500	49.000	7.000
	Priacanthidae	-	-	-	-	-	-
	Scaridae	7.333	20.500	9.000	5.500	5.500	9.000
	Sciaenidae	-	-	-	-	-	-
	Scombridae	-	-	-	-	-	-
	Scorpaenidae	-	-	-	-	0.500	-
	Serranidae	0.667	-	0.500	0.500	2.000	1.500
	Sparidae	-	0.500	-	-	-	-
	Sphyraenidae	-	-	1.000	-	0.500	0.500
	Tetraodontidae	0.333	-	-	-	-	-

Table 6. Mean fish density from RVC diver surveys according to Family and Sampling Date for Western Dry Rocks (Open, no management designation during this sampling). [Note: WDR closed to fishing effective April 1, 2021 to July 31, 2021 to facilitate spawning of certain finfish)].

Western Dry Rocks	Feb-17	May-17	July-17	Dec-17	Jun-18	Sep-18	Dec-18
Acanthuridae	11.667	5.800	14.000	13.000	5.000	12.500	51.500
Apogonidae	-	-	-	-	-	-	-
Aulostomidae	-	-	-	-	-	-	-
Carangidae	6.667	2.400	50.000	25.000	-	21.500	-
Centropomidae	-	-	-	0.250	-	-	-
Chaetodontidae	2.000	2.400	-	3.500	1.000	1.000	-
Dasyatidae	-	-	-	-	-	-	-
Echeneidae	-	-	-	-	-	-	-
Ephippidae	-	-	-	-	-	-	-
Gerreidae	-	-	-	-	-	-	-
Ginglymostomatidae	-	-	-	-	-	-	-
Gobiidae	0.667	0.200	-	-	-	-	-
Grammatidae	-	-	-	-	-	-	-
Haemulidae	5.000	3.400	2.000	21.250	12.500	2.000	100.500
Holocentridae	0.333	0.200	-	0.500	1.500	-	2.000
Kyphosidae	-	5.600	12.000	0.500	-	-	-
Labridae	68.667	43.800	22.000	61.500	19.500	17.000	23.500
Lutjanidae	12.667	9.600	11.000	7.500	13.000	0.500	1.500
Monacanthidae	-	-	-	-	-	0.500	0.500
Mullidae	0.333	-	-	-	-	-	4.000
Muraenidae	-	-	-	-	-	-	-
Ostraciidae	-	0.400	-	-	-	0.500	-
Palinuridae	-	-	-	-	-	-	-
Pomacanthidae	37.000	23.000	27.000	22.750	10.500	45.500	11.500
Priacanthidae	0.333	-	-	-	-	-	-
Scaridae	11.333	6.400	7.000	6.250	4.500	6.500	8.500
Sciaenidae	-	-	-	-	-	-	-
Scombridae	-	-	-	-	1.000	-	-
Scorpaenidae	-	-	-	-	-	-	-
Serranidae	0.667	0.600	-	-	-	1.000	1.500
Sparidae	-	-	-	0.750	-	-	0.500
Sphyraenidae	0.333	0.200	-	-	-	-	0.500
Tetraodontidae	0.333	-	-	-	-	-	-

Table 5. Mean fish density from RVC diver surveys according to Family and Sampling Date for Western Sambo (Ecological Reserve, Sanctuary Preservation Area, ER SPA)

Western Sambo (ER_SPA)	Feb-17	May-17	July-17	Dec-17	Jun-18	Sep-18	Dec-18
Acanthuridae	10.000	2.500	4.500	21.000	2.500	1.500	1.500
Apogonidae	-	-	-	-	-	-	-
Aulostomidae	-	-	-	-	-	-	-
Carangidae	6.000	1.000	-	1.500	-	0.500	0.500
Centropomidae	-	-	-	1.000	-	-	-
Chaetodontidae	-	0.500	1.000	3.000	2.000	5.500	1.500
Dasyatidae	-	-	-	-	-	-	-
Echeneidae	-	-	-	-	-	-	-
Ephippidae	-	-	-	-	-	-	-
Gerreidae	-	-	-	-	-	-	-
Ginglymostomatidae	-	-	-	-	-	-	-
Gobiidae	-	-	-	-	0.500	-	-
Grammatidae	-	-	-	-	-	-	-
Haemulidae	5.000	0.500	1.500	0.500	0.500	0.500	46.000
Holocentridae	-	-	-	-	-	-	0.500
Kyphosidae	-	-	-	-	-	1.000	-
Labridae	100.000	49.500	101.500	27.000	20.500	8.000	26.500
Lutjanidae	12.000	5.000	3.500	31.000	4.000	6.500	85.500
Monacanthidae	-	-	-	-	-	-	-
Mullidae	-	-	-	0.500	-	-	1.000
Muraenidae	-	-	-	0.500	1.000	-	-
Ostraciidae	-	-	-	-	-	-	-
Palinuridae	1.000	-	-	-	0.500	-	-
Pomacanthidae	92.000	20.000	23.000	6.500	8.500	8.000	22.500
Priacanthidae	-	-	-	-	-	-	-
Scaridae	18.000	5.000	5.000	12.000	3.000	8.000	5.500
Sciaenidae	-	-	-	-	3.000	-	-
Scombridae	-	-	0.500	-	-	-	-
Scorpaenidae	-	-	-	-	-	-	-
Serranidae	-	1.500	-	-	0.500	0.500	1.500
Sparidae	-	-	-	0.500	-	0.500	1.000
Sphyraenidae	-	-	-	0.500	-	-	0.500
Tetraodontidae	-	-	-	-	-	-	-

Table X. Mean fish density from RVC diver surveys according to Family and Sampling Date for Nine Foot Stake (Open, no management designation).

Nine Foot Stake	Feb-17	May-17	July-17	Dec-17	Jun-18	Sep-18	Dec-18
Acanthuridae	4.000	2.000	3.000	19.000	0.500	1.000	12.000
Apogonidae	-	-	-	-	-	-	-
Aulostomidae	-	-	-	-	-	-	-
Carangidae	-	3.500	-	-	-	21.500	1.500
Centropomidae	-	-	-	0.500	-	-	-
Chaetodontidae	-	4.000	1.500	5.500	2.000	2.000	1.500
Dasyatidae	-	-	-	-	-	-	-
Echeneidae	-	-	-	-	-	-	0.500
Ephippidae	-	-	-	-	-	-	-
Gerreidae	-	-	-	-	-	-	-
Ginglymostomatidae	-	-	-	-	-	-	0.500
Gobiidae	-	-	-	-	0.500	-	-
Grammatidae	-	-	-	-	-	-	-
Haemulidae	8.000	1.500	15.500	2.500	25.000	39.000	109.000
Holocentridae	-	2.000	4.000	0.500	2.500	2.500	6.000
Kyphosidae	-	5.000	12.500	-	-	0.500	13.000
Labridae	34.000	24.000	79.500	18.000	8.500	2.000	9.500
Lutjanidae	9.000	27.500	7.500	6.500	9.500	46.500	9.000
Monacanthidae	-	-	-	-	-	-	-
Mullidae	-	-	3.000	-	0.500	0.500	1.000
Muraenidae	-	-	-	-	-	-	-
Ostraciidae	-	-	0.500	-	-	-	0.500
Palinuridae	1.000	-	-	-	-	-	-
Pomacanthidae	15.000	33.000	119.500	20.500	4.500	13.000	6.500
Priacanthidae	-	-	-	-	-	-	-
Scaridae	9.000	10.500	8.500	7.000	2.000	1.500	2.500
Sciaenidae	-	-	-	-	-	-	-
Scombridae	-	-	-	-	-	-	-
Scorpaenidae	-	-	-	-	-	-	-
Serranidae	1.000	0.500	0.500	0.500	-	1.000	0.500
Sparidae	-	-	-	-	0.500	1.000	-
Sphyraenidae	-	0.500	-	-	-	0.500	0.500
Tetraodontidae	-	-	0.500	-	1.500	-	-

Table X. Mean fish density from RVC diver surveys according to Family and Sampling Date for Number 1 Marker (Open, no management designation).

Number One Marker	May-17	July-17	Dec-17	Jun-18
Acanthuridae	17.000	11.000	1.000	2.000
Apogonidae	-	-	-	-
Aulostomidae	1.000	-	-	-
Carangidae	3.000	0.500	-	15.000
Centropomidae	-	-	1.000	-
Chaetodontidae	2.500	1.500	0.500	-
Dasyatidae	-	-	-	-
Echeneidae	-	-	-	-
Ephippidae	-	-	-	-
Gerreidae	-	-	-	-
Ginglymostomatidae	0.500	-	-	-
Gobiidae	-	-	-	-
Grammatidae	-	-	-	-
Haemulidae	19.000	24.000	11.500	2.000
Holocentridae	-	-	0.500	-
Kyphosidae	0.500	1.000	0.500	-
Labridae	58.000	90.500	18.000	18.000
Lutjanidae	1.000	10.000	5.000	38.000
Monacanthidae	-	-	-	-
Mullidae	-	-	-	-
Muraenidae	-	-	-	-
Ostraciidae	-	0.500	-	-
Palinuridae	-	-	0.500	-
Pomacanthidae	75.000	75.000	10.000	2.000
Priacanthidae	-	-	-	-
Scaridae	4.500	7.500	5.500	1.000
Sciaenidae	-	0.500	4.000	-
Scombridae	-	0.500	-	-
Scorpaenidae	-	-	1.000	-
Serranidae	-	-	-	0.500
Sparidae	1.000	-	0.500	-
Sphyraenidae	0.500	-	-	-
Tetraodontidae	-	-	-	-